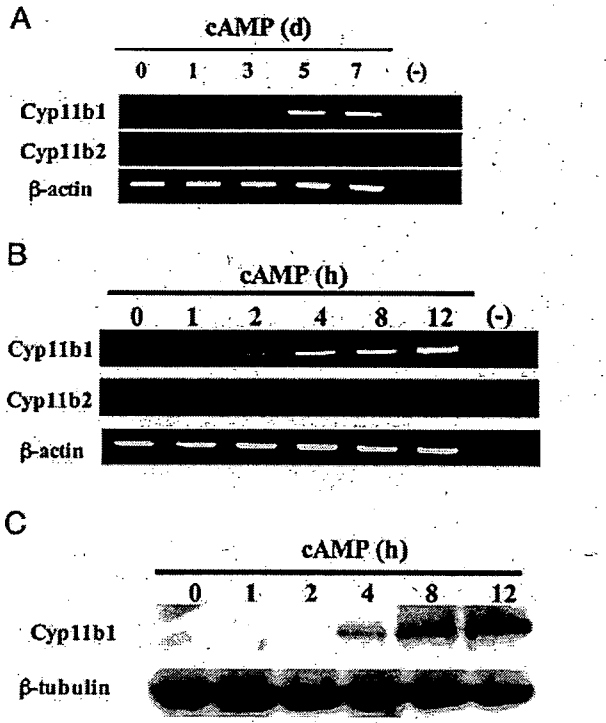

FIG. 1. Time-dependent induction of Cyp11b1 mRNA (A and B) and protein (C) by cAMP in mesenchymal stem cells (A) and MA10 cells (B and C). A, Murine mesenchymal stem cells stably transfected with an SF-1-expression vector were cultured and treated with 8-bromoadenosine-cAMP for the indicated times. mRNA levels of each gene were analyzed by RT-PCR. B and C, MA10 cells were treated with cAMP for the indicated times. C, Western blot analyses were performed with antibodies against Cyp11b1 and β-tubulin using the same lysates.

females, with much higher concentrations in the males at all times (0, 24, 48 h). The hCG treatment also elevated the 11-KT levels, but surprisingly, they were almost the same in both sexes. Thus, much higher conversion of 11-KT from testosterone seemed to occur in the ovary.

After the 11β-hydroxylation, 11-KT is produced by the actions of 11β-HSD (Fig. 4A). Two isoforms of 11β-HSD exist in mammals and have reverse activity *in vivo*; type I enzyme dominantly acts as a reductase and type II exhibits only an oxidative activity. It is possible that the expression pattern of the two isoforms in gonads may determine sexual dimorphism with respect to the conversion of testosterone to 11-KT. Therefore, we investigated the expression of the 11β-HSDs in the testis and ovary (Fig. 4B). In contrast to Cyp11b1, expression levels of 11β-HSDs, Hsd11b1 and Hsd11b2, were not affected by the hCG treatment. Hsd11b1 mRNA was expressed at higher levels in the testis than the ovary, whereas Hsd11b2 mRNA was expressed at very high levels in the ovary as reported previously (13). Only ovarian Hsd11b2 protein was detected by Western blot analysis (Fig. 4C). Immunohistochemistry showed that Hsd11b2 protein was expressed mainly in the theca cells (Fig. 4D). Using the same antibody, specific staining was not detected in the testis (data not shown). These results indicate that sexual dimorphic expression of Hsd11b2 enzyme causes the higher conversion of testosterone into 11-KT in the female.

The effects of 11-KT and other androgen on androgen receptor (AR) activation

To investigate whether 11-KT is an effective ligand of mammalian AR, we compared the androgen-dependent transcriptional activity of 11-KT with various androgens using the luciferase reporter system (Fig. 5). DHT activated AR-mediated transcription in a dose-dependent manner from 10^{-10} M. 11-KT was as effectively strong as testosterone, although to a lesser extent than DHT. Androstenedione and 11OH-testosterone were the poor activators.

AR is exclusively expressed in the granulosa cells in the ovary (27). Because androgens can be converted to estrogens by aromatase, they could act as not only androgen but also the precursors of estrogens in these cells. Therefore, we compared androgenic activity of the aromatizable testosterone with that of the nonaromatizable 11-KT by their transcriptional activities through AR in the granulosa-like tumor KGN cells (Fig. 6). Both androgens significantly activated the AR-mediated transcription from 10^{-10} M in these cells. However, 11-KT showed significant higher activity than testosterone at 10^{-10} and 10^{-9} M ($P < 0.01$). Such a difference was blunted by the addition of aromatase inhibitors, fadrozole (Fig. 6) or anastrozole (data not shown). A significant difference was not observed at 10^{-8} M, probably because unconverted testosterone levels were high enough to exert the maximum response at this concentration. These results suggest that the conversion from testosterone to 11-KT may have a role in maintaining the androgenic activity caused by testosterone in granulosa cells by preventing aromatization.

Discussion

In this study, we demonstrated that the metabolic pathway producing 11-KT in the fish gonad is also conserved in murine gonads, although there is a marked difference in the production pattern in the gonads. In fish, this pathway is dominant in males (testis) and causes much higher 11-KT levels when compared with females. 11-KT is necessary for the male sexual phenotype and spermatogenesis in fish testis. In addition, it induces female-to-male sex reversal in some teleost species (9, 10). In contrast to fish, this pathway is dominant in female (ovary) mice.

In mammals, it is believed that the steroid 11β-hydroxylase, CYP11B1 or Cyp11b1, is an adrenal-specific gene and is responsible for the last step of glucocorticoid biosynthesis. However, Cyp11b1 was induced by cAMP treatment in the Leydig-like cells made from murine bone marrow-derived mesenchymal stem cells as well as in Leydig cell tumor-derived MA10 cells. Supporting the physiological relevance of this phenomenon, it was also induced *in vivo* by hCG treatment in testicular Leydig cells and ovarian theca cells. In addition, Wang *et al.* (3) reported that Cyp11b1 was expressed in rat testis. These results indicate that 11β-hydroxylase (Cyp11b1) is not an adrenal-specific gene. Recently Val *et al.* (28) reported that adrenal-like cells exist in the embryonic murine testis, and they respond to both ACTH and hCG that leads to the expression of Cyp11b1. However, it is unlikely that adrenal-like cells in murine gonads can explain our present observation because adrenal-like cells are presently unknown in the murine ovary, and induction of

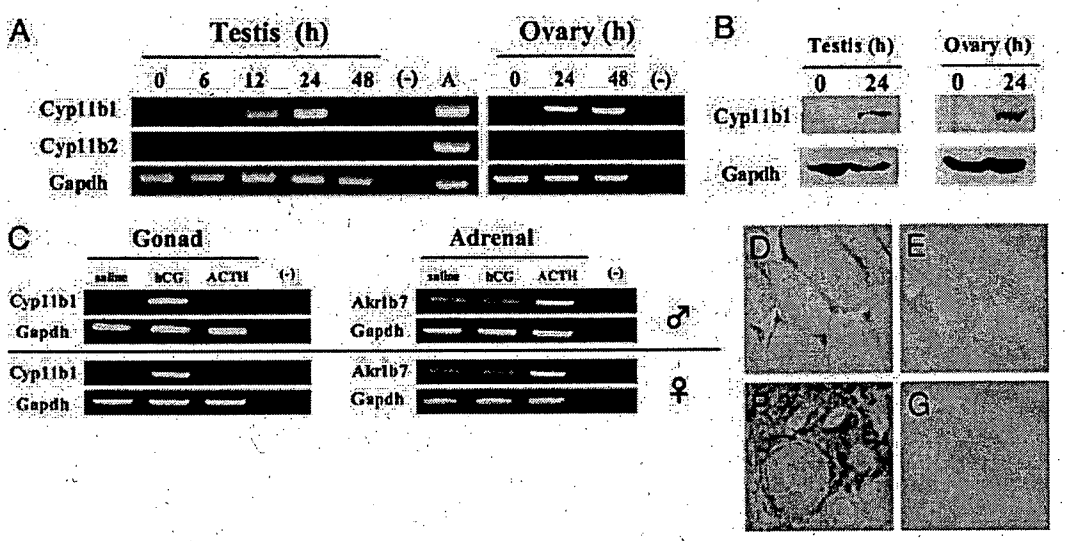

FIG. 2. Induction of Cyp11b1 mRNA and protein by hCG in murine testes and ovaries. Animals were treated with hCG, and gonads were removed at indicated times (A and B). A, mRNA levels of each gene were analyzed by RT-PCR. Lane A represents an adrenal. B, Western blot analyses were performed with antibodies against Cyp11b1 and Gapdh using the same lysates. C, Animals were treated with saline, hCG, or ACTH, and tissues were removed at 16 h. mRNA levels of each gene were analyzed by RT-PCR. D–G, Localization of Cyp11b1 protein in the murine gonad. Testes or ovaries from mice treated with hCG for 24 h were used. Positive staining for Cyp11b1 was observed in testicular Leydig cells (D) and ovarian theca cells (F). No staining was observed in control sections incubated with nonimmune serum (E and G).

Cyp11b1 was observed in almost all populations of Leydig or theca cells. In addition, Cyp11b1 mRNA was not detected in gonads of ACTH-treated animals because O'Shaughnessy *et al.* (29) reported the deficiency of response to ACTH stimulation in adult Leydig cells. Rather, these results suggest that testicular Leydig cells and ovarian theca cells have a capacity to express Cyp11b1, as in the case of adrenal-like cells.

As we reported previously (23), much longer times (1–5 d) were necessary to induce all the steroidogenic enzymes by cAMP treatment in mesenchymal stem cells (MSCs) (including KUM9) than steroidogenic cell lines including MA10 (1–8 h). Then we speculated that the cAMP treatment in MSCs induced the differentiation of stem cells into steroidogenic linage in MSCs, whereas it induces the transactivation of steroidogenic enzymes in steroidogenic cell lines. Supporting this assumption, Cyp11b1 had been induced by retreatment of the cAMP in MSC-derived cells as fast as in the MA10 cells after 7 d cAMP treatment and ensuring depletion of the cAMP.

Considerable work has been done on the mechanisms that regulate transcription of human and bovine 11β-hydroxylase genes, CYP11B1 and CYP11B, respectively. Transcription factors, steroidogenic factor 1 (SF-1) (also known as Ad4BP) and cAMP response element-binding protein are known to play a vital role in both species (30–32). The model also seems to be applicable to the transcriptional regulation of murine Cyp11b1 because it is induced in nonsteroidogenic mesenchymal stem cells by the stable transfection of SF-1 and the treatment of cAMP (23, 33), although its promoter analysis is not yet reported. SF-1 is essential for the development of the adrenal gland and gonad and sexual differentiation (34–36). It is expressed in the adrenal cortex, testicular Leydig and Sertoli cells, ovarian theca and granulosa cells, pituitary gonadotroph, hypothalamus, and spleen. SF-1 is a member of the nuclear receptor superfamily and regulates the cell-specific expression of a variety of different genes involved in steroidogenesis including a number of steroid hydroxylases (34–37). The expression pattern of SF-1 during urogenital development suggested that adrenal and gonadal cells are derived from common precursor cell populations (38). Therefore, it is conceivable that Cyp11b1 mRNA is induced by LH/hCG treatment in gonadal steroidogenic cells as well as by ACTH treatment in the adrenal gland. However, other adrenal-specific factors should be involved in the transcription of Cyp11b1 because the expression levels were much higher in adrenocortical cells than gonadal cells, even after hCG or cAMP treatment. Further studies will be necessary to understand the regulatory mechanisms of the Cyp11b1 gene expression.

Because the substrate precursors for glucocorticoid are not produced in the gonad due to the deficiency of Cyp21, Cyp11b1 may be involved in steroid metabolism, other than glucocorticoid synthesis in the gonad. In eel testis, 11β-hydroxylase is induced by hCG treatment and contributes to the production of the fish androgen 11-KT (4, 26). This was also observed in murine gonads, with the elevation of the plasma 11-KT levels by hCG treatment. It is likely that 11-KT is not only a teleost androgen but also a mammalian androgen. This is supported by the findings that 11-KT was able to activate mammalian AR-mediated transcription.

There is, however, a marked difference between teleosts and mammals with respect to the production of 11KT. 11-KT is a major androgen in most male teleost species and was found at much higher concentrations in male plasma than in female, whereas this is usually not the case for testosterone (39, 40). In teleosts, 11-KT is involved in the many male reproductive processes, such as spermatogenesis (6, 7), development of secondary sex characteristics (8, 9), and modulation of behavior (9). In addition, it eventually induces

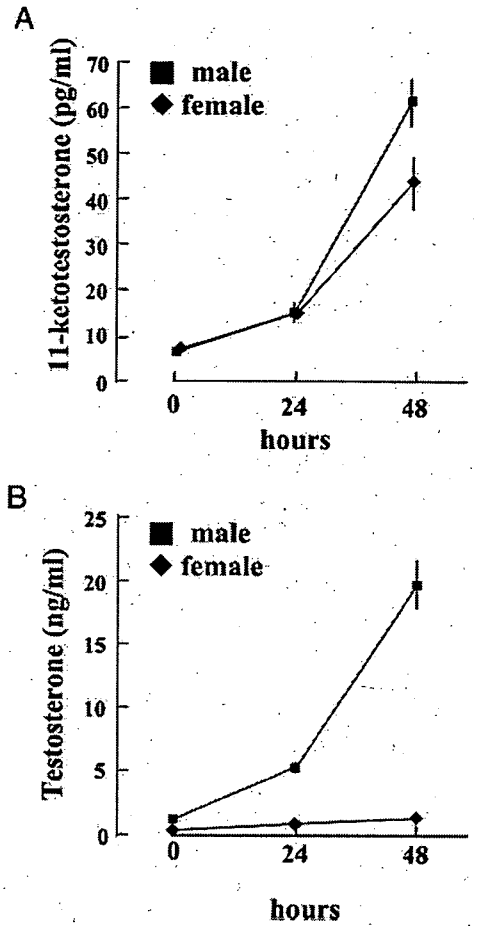

FIG. 3. Concentrations of serum androgens in mice treated with hCG. Serum 11-KT (A) and testosterone (B) concentrations in male (■) and female (◆) mice treated with hCG at indicated times. Data for each point are from five animals (means and SEM).

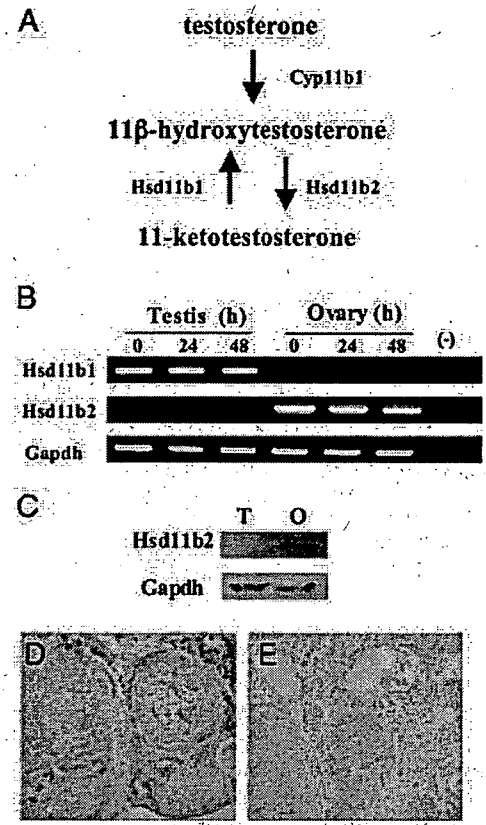

FIG. 4. The expression and localization of the 11β-HSDs in the murine gonad. A, The enzymes and pathways involved in the synthesis of 11-KT. B, mRNA levels of each gene in gonads treated with hCG for indicated times were analyzed by RT-PCR. C, Immunoblot of Hsd11b2 and Gapdh proteins in testis (T) and ovary (O) using the same lysates. Localization of Hsd11b2 protein in the ovary (D and E). Positive staining for Hsd11b2 was observed in theca cells (D). No staining was observed in control sections incubated with nonimmune serum (E).

female-to-male sex reversal in some species (10). In contrast to teleosts, murine plasma 11-KT concentrations were at similar levels in both sexes, whereas testosterone levels were much higher in males. Such a difference between these vertebrates implies a difference in sexual dimorphic expression of the enzymes involving the conversion of 11-KT in their gonads. In teleost gonads, P450 11β is exclusively expressed in the testis (41–43), whereas murine Cyp11b1 was induced by hCG both in the testis and ovary at similar levels. By contrast, teleost 11β-HSD2 is abundantly expressed in the testis (20, 21), whereas murine Hsd11b2 was expressed more highly in the ovary. These results indicate that the 11-KT production pathway is conserved between teleosts and mammals, although its major physiological role(s) may have become different during their evolution.

Wang *et al.* (3) reported that 11β-hydroxysteroids or 11-ketosteroids were involved in the regulation of 11β-HSD activity in Leydig cells. 11β-hydroxysteroids were efficient inhibitors of Hsd11b1 dehydrogenase activity, whereas 11-keto compounds were effective as inhibitors of oxidoreductase activity. 11β-HSDs in Leydig cells convert active glucocorticoids to the inert 11-keto form, thereby playing a protective role in blunting the suppressive effects of glucocorticoid on Leydig cell steroidogenesis. Therefore, 11-KT is a possible controller of the testicular steroidogenesis via regulating the activity of 11β-HSDs. This may also be true in the ovarian steroidogenesis. As in the case of testicular Leydig cells, ovarian steroidogenesis is also inhibited by glu-

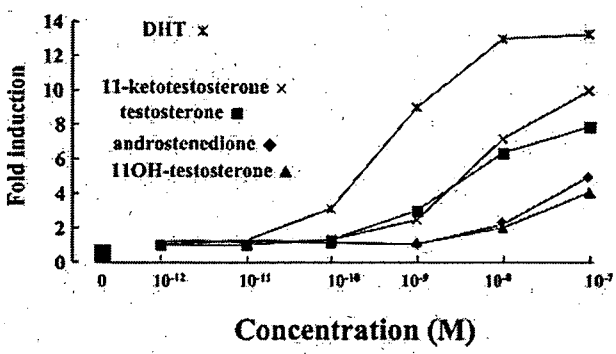

FIG. 5. Activation of mammalian AR by various androgens. CV-1 cells were transiently transfected with the ARE-Luc vector together with an AR expression vector. After 24 h after transfection, cells were incubated with or without increasing concentrations of various androgens for 24 h. Data are shown as the mean ± SEM values of at least four independent assays.

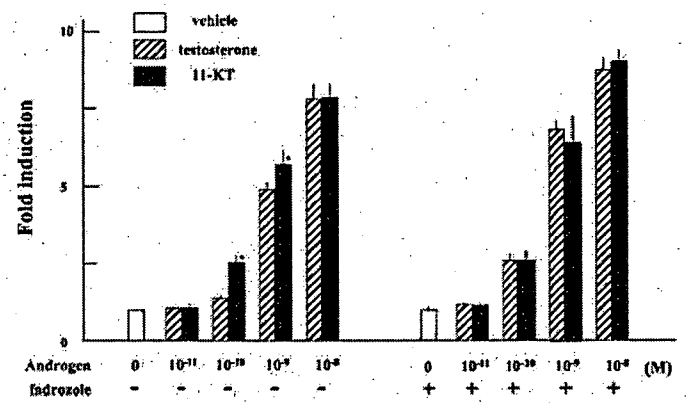

FIG. 6. Comparison of AR-mediated transactivation by testosterone and 11-KT in granulosa like-tumor KGN cells. KGN cells were transiently transfected with the slp-ARU-tk/Luc vector together with an AR expression vector. After 24 h after transfection, cells were incubated with or without androgens and fadrozole (1 μM) for 24 h. Data are shown as the mean ± SEM values of at least four independent assays. *, Significant difference in transactivation between testosterone and 11-KT ($P < 0.01$).

cocorticoid (44, 45). In addition, higher expression of Hsd11b2 in the ovary suggests that ovarian Hsd11b2 may regulate the ovarian steroidogenesis by limiting the accessibility of active glucocorticoid to ovarian glucocorticoid receptors via 11-KT production. It also suggests that the ovary may be a new target organ of the mineralocorticoid-mineralocorticoid receptor pathway. Recently Fru *et al.* (46) reported that, compared with the glucocorticoid actions, mineralocorticoid stimulates progesterone synthesis by periovulatory granulosa cells in macaques. Therefore, it is conceivable that the complex steroid metabolism and signaling including androgen may regulate ovarian steroidogenesis.

The induction of 11KT by gonadotropin treatment suggests that 11-KT is also involved in folliculogenesis. In fact, androgen receptor KO (ArKO) female mice showed a subfertile phenotype, resulting from the impairment of ovulation and corpus lutea formation (27, 47). Because ovarian AR is exclusively expressed in granulosa cells (27), those phenotypes in ArKO mice suggest that androgens induce genes associated with folliculogenesis in granulosa cells. Our results in KGN cells suggest that conversion from testosterone to 11-KT may have a role in maintaining the androgenic activity caused by testosterone in granulose cells because it can efficiently induce AR-regulated genes in these cells. Shiina *et al.* (27) reported that Kit ligand is the direct downstream target of AR, and its down-regulation in ArKO mice is the cause of premature ovarian failure. Future studies will be necessary to investigate the relationship between Kit ligand and 11-KT-AR pathway in the ovary.

In summary, we reported that the metabolic pathway producing 11-KT, a major teleost androgen, was conserved in the mammalian gonad, although it was more active in the ovary. In female eels, however, 11-KT synthesis and levels fluctuated during oogenesis and follicular maturation (48). Therefore, 11-KT production and AR signaling in female might be conserved from teleosts to mammals, even though 11-KT has been replaced by DHT in male during evolution.

Acknowledgments

We are grateful to Drs. S. Kato, M. Nakai, H. Takemori, T. Yanase, and M. Ascoli for providing the materials. We also thank Ms. Y. Inoue, K. Matsuura, and H. Fujii for technical assistance.

Received July 24, 2007. Accepted December 19, 2007.

Address all correspondence and requests for reprints to: Kaoru Miyamoto, Department of Biochemistry, Faculty of Medical Sciences, University of Fukui, Shimoaizuki, Matsuoka, Eiheiji-cho, Fukui 910-1193, Japan. E-mail: kmiyamot@u-fukui.ac.jp.

This work was supported in part by a grant from the Smoking Research Foundation, Kanzawa Medical Research Foundation, 21st Century Center of Excellence Program (Medical Science), and Research and Education Program for Life Science.

Disclosure Statement: All authors (T.Y., M.U., Y.I., T.M., T.S., T.Ka., T.Ki., A.U., K.M.) have nothing to declare.

References

1. **Domalik LJ, Chaplin DD, Kirkman MS, Wu RC, Liu WW, Howard TA, Seldin MF, Parker KL** 1991 Different isozymes of mouse 11β-hydroxylase produce mineralocorticoids and glucocorticoids. Mol Endocrinol 5:1853–1861
2. **Ogishima T, Suzuki H, Hata J, Mitani F, Ishimura Y** 1992 Zone-specific expression of aldosterone synthase cytochrome P-450 and cytochrome P-45011β in rat adrenal cortex: histochemical basis for the functional zonation. Endocrinology 130:2971–2977
3. **Wang GM, Ge RS, Latif SA, Morris DJ, Hardy MP** 2002 Expression of 11β-hydroxylase in rat Leydig cells. Endocrinology 143:621–626
4. **Jiang JQ, Kobayashi T, Ge W, Kobayashi H, Tanaka M, Okamoto M, Nonaka Y, Nagahama Y** 1996 Fish testicular 11β-hydroxylase: cDNA cloning and mRNA expression during spermatogenesis. FEBS Lett 397:250–252
5. **Jiang JQ, Young G, Kobayashi T, Nagahama Y** 1998 Eel (*Anguilla japonica*) testis 11β-hydroxylase gene is expressed in interrenal tissue and its product lacks aldosterone synthesizing activity. Mol Cell Endocrinol 146:207–211
6. **Miura T, Yamauchi K, Takahashi H, Nagahama Y** 1991 Hormonal induction of all stages of spermatogenesis *in vitro* in the male Japanese eel (*Anguilla japonica*). Proc Natl Acad Sci USA 88:5774–5778
7. **Nagahama Y** 1994 Endocrine regulation of gametogenesis in fish. Int J Dev Biol 38:217–229
8. **Mayer I, Borg B, Schulz R** 1990 Seasonal changes in and effect of castration/androgen replacement on the plasma levels of five androgens in the male three-spined stickleback, *Gasterosteus aculeatus L.* Gen Comp Endocrinol 79:23–30
9. **Kobayashi M, Nakanishi T** 1999 11-Ketotestosterone induces male-type sexual behavior and gonadotropin secretion in gynogenetic crucian carp, *Carassius auratus langsdorfii.* Gen Comp Endocrinol 115:178–187
10. **Cardwell JR, Liley NR** 1991 Hormonal control of sex and color change in the stoplight parrotfish, *Sparisoma viride.* Gen Comp Endocrinol 81:7–20
11. **Curnow KM, Slutsker L, Vitek J, Cole T, Speiser PW, New MI, White PC, Pascoe L** 1993 Mutations in the CYP11B1 gene causing congenital adrenal hyperplasia and hypertension cluster in exons 6, 7, and 8. Proc Natl Acad Sci USA 90:4552–4556
12. **Karnak I, Senocak ME, Göğüçs S, Büyükpamukçu N, Hiçsönmez A** 1999 Testicular enlargement in patients with 11-hydroxylase deficiency. J Pediatr Surg 32:756–758
13. **Condon J, Ricketts ML, Whorwood CB, Stewart PM** 1997 Ontogeny and sexual dimorphic expression of mouse type 2 11β-hydroxysteroid dehydrogenase. Mol Cell Endocrinol 127:121–128
14. **Paterson JM, Seckl JR, Mullins JJ** 2005 Genetic manipulation of 11β-hydroxysteroid dehydrogenases in mice. Am J Physiol Regul Integr Comp Physiol 289:R642–R652
15. **Draper N, Walker EA, Bujalska IJ, Tomlinson JW, Chalder SM, Arlt W, Lavery GG, Bedendo O, Ray DW, Laing I, Malunowicz E, White PC, Hewison M, Mason PJ, Connell JM, Shackleton CH, Stewart PM** 2003 Mutations in the genes encoding 11β-hydroxysteroid dehydrogenase type 1 and hexose-6-phosphate dehydrogenase interact to cause cortisone reductase deficiency. Nat Genet 34:434–439
16. **Gambineri A, Vicennati V, Genghini S, Tomassoni F, Pagotto U, Pasquali R, Walker BR** 2006 Genetic variation in 11β-hydroxysteroid dehydrogenase type 1 predicts adrenal hyperandrogenism among lean women with polycystic ovary syndrome. J Clin Endocrinol Metab 91:2295–2302
17. **White PC** 2005 Genotypes at 11β-hydroxysteroid dehydrogenase type 11B1 and hexose-6-phosphate dehydrogenase loci are not risk factors for apparent cortisone reductase deficiency in a large population-based sample. J Clin Endocrinol Metab 90:5880–5883
18. **San Millan JL, Botella-Carretero JI, Alvarez-Blasco F, Luque-Ramirez M, Sancho J, Moghetti P, Escobar-Morreale HF** 2005 A study of the hexose-6-phosphate dehydrogenase gene R453Q and 11β-hydroxysteroid dehydroge-

nase type 1 gene 83557insA polymorphisms in the polycystic ovary syndrome. J Clin Endocrinol Metab 90:4157–4162
19. **Kotelevtsev Y, Brown RW, Fleming S, Kenyon C, Edwards, CRW, Seckl JR Mullins JJ** 1999 Hypertension in mice lacking 11β-hydroxysteroid dehydrogenase type 2. J Clin Invest 103:683–689
20. **Jiang JQ, Wang DS, Senthilkumaran B, Kobayashi T, Kobayashi HK, Yamaguchi A, Ge W, Young G, Nagahama Y** 2003 Isolation, characterization and expression of 11β-hydroxysteroid dehydrogenase type 2 cDNAs from the testes of Japanese eel (*Anguilla japonica*) and Nile tilapia (*Oreochromis niloticus*). J Mol Endocrinol 31:305–315
21. **Kusakabe M, Nakamura I, Young G** 2003 11β-Hydroxysteroid dehydrogenase complementary deoxyribonucleic acid in rainbow trout: cloning, sites of expression, and seasonal changes in gonads. Endocrinology 144:2534–2545
22. **Verrijdt G, Schauwaers K, Haelens A, Rombauts W, Claessens F** 2002 Functional interplay between two response elements with distinct binding characteristics dictates androgen specificity of the mouse sex-limited protein enhancer. J Biol Chem 277:35191–35201
23. **Yazawa T, Mizutani T, Yamada K, Kawata H, Sekiguchi T, Yoshino M, Kajitani T, Shou Z, Umezawa A, Miyamoto K** 2006 Differentiation of adult stem cells derived from bone marrow stroma into Leydig or adrenocortical cells. Endocrinology 147:4104–4111
24. **Yazawa T, Mizutani T, Yamada K, Kawata H, Sekiguchi T, Yoshino M, Kajitani T, Shou Z, Miyamoto K** 2003 Involvement of cyclic adenosine 5′-monophosphate response element-binding protein, steroidogenic factor 1, and Dax-1 in the regulation of gonadotropin-inducible ovarian transcription factor 1 gene expression by follicle-stimulating hormone in ovarian granulosa cells. Endocrinology 144:1920–1930
25. **Yazawa T, Nakayama Y, Fujimoto K, Matsuda Y, Abe K, Kitano T, Abe S, Yamamoto T** 2003 Abnormal spermatogenesis at low temperatures in the Japanese red-bellied newt, *Cynops pyrrhogaster*: possible biological significance of the cessation of spermatocytogenesis. Mol Reprod Dev 66:60–66
26. **Miura T, Yamauchi K, Nagahama Y, Takahashi H** 1991 Induction of spermatogenesis in male Japanese eel, *Anguilla japonica*, by a single injection of human chorionic gonadotropin. Zool Sci 8:63–73
27. **Shiina H, Matsumoto T, Sato T, Igarashi K, Miyamoto J, Takemasa S, Sakari M, Takada I, Nakamura T, Metzger D, Chambon P, Kanno J, Yoshikawa H, Kato S** 2006 Premature ovarian failure in androgen receptor-deficient mice. Proc Natl Acad Sci USA 103:224–229
28. **Val P, Jeays-Ward K, Swain A** 2006 Identification of a novel population of adrenal-like cells in the mammalian testis. Dev Biol 299:250–256
29. **O'Shaughnessy PJ, Fleming LM, Jackson G, Hochgeschwender U, Reed P, Baker PJ** 2003 Adrenocorticotropic hormone directly stimulates testosterone production by the fetal and neonatal mouse testis. Endocrinology 144:3279–3284
30. **Wang XL, Bassett M, Zhang Y, Yin S, Clyne C, White PC, Rainey WE** 2000 Transcriptional regulation of human 11β-hydroxylase (hCYP11B1). Endocrinology 141:3587–3594
31. **Takayama K, Morohashi K, Honda S, Hara N, Omura T** 1994 Contribution of Ad4BP, a steroidogenic cell-specific transcription factor, to regulation of the human CYP11A and bovine CYP11B genes through their distal promoters. J Biochem (Tokyo) 116:193–203
32. **Rainey WE** 1999 Adrenal zonation: clues from 11β-hydroxylase and aldosterone synthase. Mol Cell Endocrinol 151:151–160
33. **Gondo S, Yanase T, Okabe T, Tanaka T, Morinaga H, Nomura M, Goto K, Nawata H** 2004 SF-1/Ad4BP transforms primary long-term cultured bone marrow cells into ACTH-responsive steroidogenic cells. Genes Cells 9:1239–1247
34. **Ikeda Y, Lala DS, Luo X, Kim E, Moisan MP, Parker KL** 1993 Characterization of the mouse FTZ-F1 gene, which encodes a key regulator of steroid hydroxylase gene expression. Mol Endocrinol 7:852–860
35. **Morohashi K** 1999 Gonadal and extragonadal functions of Ad4BP/SF-1: developmental aspects. Trends Endocrinol Metab 10:169–173
36. **Parker KL, Schimmer BP** 1997 Steroidogenic factor 1: a key determinant of endocrine development and function. Endocr Rev 18:361–377
37. **Morohashi K, Iida H, Nomura M, Hatano O, Honda S, Tsukiyama T, Niwa O, Hara T, Takakusu A, Shibata Y, Omura T** 1994 Functional difference between Ad4BP and ELP, and their distributions in steroidogenic tissues. Mol Endocrinol 8:643–653
38. **Morohashi K** 1997 The ontogenesis of the steroidogenic tissues. Genes Cells 2:95–106
39. **Borg B** 1994 Androgens in teleost fishes. Comp Biochem Physiol 109:219–245
40. **Lokman PM, Harris B, Kusakabe M, Kime DE, Schulz RW, Adachi S, Young G** 2002 11-Oxygenated androgens in female teleosts: prevalence, abundance, and life history implications. Gen Comp Endocrinol 129:1–12
41. **Liu S, Govoroun M, D'Cotta H, Ricordel MJ, Lareyre JJ, McMeel OM, Smith T, Nagahama Y, Guiguen Y** 2000 Expression of cytochrome P450(11β) (11β-hydroxylase) gene during gonadal sex differentiation and spermatogenesis in rainbow trout, *Oncorhynchus mykiss*. J Steroid Biochem Mol Biol 75:291–298
42. **Yokota H, Abe T, Nakai M, Murakami H, Eto C, Yakabe Y** 2005 Effects of 4-tert-pentylphenol on the gene expression of P450 11β-hydroxylase in the gonad of medaka (*Oryzias latipes*). Aquat Toxicol 71:121–132
43. **Socorro S, Martins RS, Deloffre L, Mylonas CC, Canario AV** 2007 A cDNA for European sea bass (*Dicentrachus labrax*) 11β-hydroxylase: gene expression during the thermosensitive period and gonadogenesis. Gen Comp Endocrinol 150:164–173
44. **Hsueh AJ, Erickson GF** 1978 Glucocorticoid inhibition of FSH-induced estrogen production in cultured rat granulosa cells. Steroids 32:639–648
45. **Valli G, Sudha S, Ravi Sankar B, Govindarajulu P, Srinivasan N** 2000 Altered corticosterone status impairs steroidogenesis in the granulosa and thecal cells of Wistar rats. J Steroid Biochem Mol Biol 73:153–158
46. **Fru KN, VandeVoort CA, Chaffin CL** 2006 Mineralocorticoid synthesis during the periovulatory interval in macaques. Biol Reprod 75:568–574
47. **Hu YC, Wang PH, Yeh S, Wang RS, Xie C, Xu Q, Zhou X, Chao HT, Tsai MY, Chang C** 2004 Subfertility and defective folliculogenesis in female mice lacking androgen receptor. Proc Natl Acad Sci USA 101:11209–11214
48. **Matsubara H LP, Senaha A, Kazeto Y, Ijiri S, Kambegawa A, Hirai T, Youg G, Todo T, Adachi S, Yamauchi K** 2003 Synthesis and possible function of 11-ketotestosterone during oogenesis in eel (*Anguilla japonica*). Fish Physiol Biochem 28:353–354

Endocrinology **is published monthly by The Endocrine Society (http://www.endo-society.org), the foremost professional society serving the endocrine community.**

In Vitro Cell.Dev.Biol.—Animal (2007) 43:129–138
DOI 10.1007/s11626-007-9021-9

Chromosomal instability in human mesenchymal stem cells immortalized with human papilloma virus E6, E7, and hTERT genes

Masao Takeuchi · Kikuko Takeuchi · Arihiro Kohara · Motonobu Satoh · Setsuko Shioda · Yutaka Ozawa · Azusa Ohtani · Keiko Morita · Takashi Hirano · Masanori Terai · Akihiro Umezawa · Hiroshi Mizusawa

Received: 25 January 2007 / Accepted: 27 March 2007 / Published online: 21 May 2007 / Editor: J. Denry Sato

Abstract Human mesenchymal stem cells (hMSCs) are expected to be an enormous potential source for future cell therapy, because of their self-renewing divisions and also because of their multiple-lineage differentiation. The finite lifespan of these cells, however, is a hurdle for clinical application. Recently, several hMSC lines have been established by immortalized human telomerase reverse transcriptase gene (hTERT) alone or with hTERT in combination with human papillomavirus type 16 E6/E7 genes (E6/E7) and human proto-oncogene, Bmi-1, but have not so much been characterized their karyotypic stability in detail during extended lifespan under in vitro conditions. In this report, the cells immortalized with the hTERT gene alone exhibited little change in karyotype, whereas the cells immortalized with E6/E7 plus hTERT genes or Bmi-1, E6 plus hTERT genes were unstable regarding chromosome numbers, which altered markedly during prolonged culture. Interestingly, one unique chromosomal alteration was the preferential loss of chromosome 13 in three cell lines, observed by fluorescence in situ hybridization (FISH) and comparative-genomic hybridization (CGH) analysis. The four cell lines all maintained the ability to differentiate into both osteogenic and adipogenic lineages, and two cell lines underwent neuroblastic differentiation. Thus, our results were able to provide a step forward toward fulfilling the need for a sufficient number of cells for new therapeutic

M. Takeuchi (✉) · K. Takeuchi · A. Kohara · S. Shioda · Y. Ozawa · A. Ohtani · H. Mizusawa
Division of Bioresources,
National Institute of Biomedical Innovation,
Osaka 567-0085, Japan
e-mail: takeuchim@nibio.go.jp

K. Takeuchi
e-mail: takeuchik@nibio.go.jp

A. Kohara
e-mail: kohara@nibio.go.jp

S. Shioda
e-mail: shioda@nibio.go.jp

Y. Ozawa
e-mail: ozaway@nibio.go.jp

A. Ohtani
e-mail: aohtani@nibio.go.jp

H. Mizusawa
e-mail: mizusawa@nibio.go.jp

M. Satoh
Health Science Research Resources Bank,
Osaka 590-0535, Japan
e-mail: satoh@osa.jhsf.or.jp

K. Morita · T. Hirano · A. Umezawa
National Research Institute for Child Health and Development,
Tokyo 157-8535, Japan

K. Morita
e-mail: morita-keiko@aist.go.jp

T. Hirano
e-mail: hirano-takashi@aist.go.jp

A. Umezawa
e-mail: umezawa@1985.jukuin.keio.ac.jp

M. Terai
Department of Reproductive Biology
and Pathology and Innovative Surgery,
National Research Institute for Child Health and Development,
Tokyo 157-8535, Japan
e-mail: terai@nch.go.jp

applications, and substantiate that these cell lines are a useful model for understanding the mechanisms of chromosomal instability and differentiation of hMSCs.

Keywords Human cord blood mesenchymal stem cell · Long-term culture · Karyotype analysis · mFISH CGH · Differentiation

Introduction

Tissue-specific stem cells in various adult tissues are known to be an important source in the regeneration of damaged tissue and maintenance of homeostasis in the tissues in which they reside. Among these stem cells, human mesenchymal stem cell (hMSC) has recently become of great interest in regenerative medicine, not only to replenish their own tissues, but also to give rise to more committed progenitor cells, which can differentiate into other tissues. MSCs in bone marrow have been shown to differentiate into several types of cell such as osteoblasts, adipocytes, chondrocytes, myocytes, and probably also neuronal cells (Okamoto et al. 2002; Takeda et al. 2004; Mori et al. 2005; Saito et al. 2005; Terai et al. 2005). Because of these properties, it is expected that hMSCs are an enormous potential source for future cell therapy. The goal of our study is to establish cell lines with long lifespan and with parental properties for clinical application. However, clinical application using these cells has been met with enormous difficulty, e.g., isolation of a cell population with specific criteria, expansion in vitro system for obtaining a sufficient number of cells without affecting their genomic characteristics and differentiation properties, and their storage in higher viability.

At present, there is a little evidence suggesting whether changes in these properties occur during expansion. Human normal MSCs have a limited capacity to replicate in the 40- to 50-population doubling level (PDL) at the most. To extend their lifespan, we have previously established human mesenchymal cell lines from human umbilical cord blood or bone marrow by immortalization with human telomerase reverse transcriptase (hTERT), human papillomavirus high-risk type 16 E6/E7 genes (HPV16E6/E7) or polycomb gene, Bmi-1 (Takeda et al. 2004; Mori et al. 2005; Terai et al. 2005).

hTERT-immortalization without affecting biological characteristics, despite extensive proliferation, has been reported in bone-marrow-derived hMSCs (Burns et al. 2005), human fibroblast (Milyavsky et al. 2003), and human keratinocyte (Harada et al. 2003), although it has been indicated that there is the possibility that prolonged culture of hTERT-immortalized fibroblasts may favor the appearance of clones carrying potentially malignant alterations (Milyavsky et al. 2003). HPV16, which encodes oncogenes (E6 and E7), can also immortalize hMSCs in vitro. Both E6 and E7 proteins act through their association with tumor suppressor gene products, p53 and retinoblastoma family members (pRb), respectively. E6 accelerates the degradation of the p53 protein, which is essential for cell arrest at the checkpoint in G_1/S and at the mitotic checkpoint when tetraploidy occurs (Cross et al. 1995), as well as at the G_2 phase under damaging conditions. E7 protein binds to pRb and abrogates the repressive function of these cell cycle regulations (Zheng et al. 2001). Thus, both p53 and pRb play a multitude of important roles in cell-cycle-progression checkpoints as reported in human keratinocytes (Patel et al. 2004), and fibroblasts (Khan et al. 1998). As a consequence, the disruption of the checkpoints that govern accurate cell division leads to abnormal segregation of chromosome and genomic instability, as shown in the cells immortalized with HPV16E6/E7 genes (Duensing et al. 2002).

In this paper, we report on the chromosomal instability and the differentiation activity during prolonged culture (cell expansion) using four mesenchymal stem cell lines. These results indicate that an umbilical cord blood-derived clone immortalized with hTERT (UCBTERT-21) showed normal karyotype for a period of 1 yr, whereas three other cell lines immortalized with HPV16E6/E7 and hTERT or HPV16E6, Bmi-1 and hTERT showed chromosomal instability but maintained the ability to differentiate.

Materials and Methods

Cell culture. Human mesenchymal stem cell lines, UCB TERT-21 (JCRB1107), UCB408E6E7TERT-33 (JCRB1110), UE6E7T-3 (JCRB1136), and UBE6T-6 (JCRB1140) were obtained from the JCRB Cell Bank (Osaka, Japan). Two of them are cell lines obtained by immortalizing human umbilical cord blood mesenchymal stem cells (UCB) with hTERT alone (UCBTERT-21; Terai et al. 2005) or with HPV16E6/E7 in combination with hTERT (UCB408E6E7TERT-33; Terai et al. 2005), and the two others are human bone-marrow-derived mesenchymal stem cell lines transformed with HPV16E6/E7 and hTERT genes (UE6E7T-3; Mori et al. 2005) or with bmi-1, HPV16E6 and hTERT genes (UBE6T-6; Takeda et al. 2004; Mori et al. 2005).

The UCBTERT-21 and UCB408E6E7TERT-33 were grown in PLUSOID-M medium (Med-Shirotori Co., Tokyo, Japan) or MSCGM BulletKit (Cambrex Co., East Rutherford, NJ). UE6E7T-3 and UBE6T-6 were cultured in POWEREDBY10 medium (Med-Shirotori Co.) or MSCGM BulletKit (Cambrex Co.); 5×10^3 cells/ml of each cell line were seeded and cultured for 7–10 d. When culture

plate was subconfluent, cells were treated with 0.25% trypsin/0.5 mM EDTA solution (both from Invitrogen, Tokyo, Japan) and replated at a density of 5×10^3 cells/ml.

All of the cells were maintained in a humidified incubator at 37° C and 5% CO_2. PDLs were calculated using the formula: PDL= log (cell output/input)/log2. At the starting cultivation, PDLs of UCBTERT-21, UCB408E6E7 TERT-33, UE6E7T-3, and UBE6T-6 were 42, 67, 60, and 56, respectively. The doubling time of the UCB408E6E7T-33 cell was 1.5 d, and that of UCBTERT-21, UE6E7T-3, or UBE6T-6 was 2.6, 2.0, or 4.0 days, respectively.

Measurement of chromosome number and fluorescence in situ hybridization. Metaphase chromosome spreads for measurement of chromosome number and fluorescence in situ hybridization (FISH) were prepared from exponential growing cells at various PDL. The cells were treated in a hypotonic solution after exposure to 0.06 μg/ml colcemid (Invitrogen, Carlsbad, CA) for 2 h and fixed in methanol/acetic acid (3:1). The cells were spread on a microscope slide.

To count the number of chromosomes, the cells were stained with DAPI (4′-6-diaminido-2-phenylindol; Vector Laboratories, Inc. Burlingame, CA) and examined under an Axioplan II imaging microscope (Carl Zeiss, GmbH) equipped with Leica QFISH software (Leica Microsystems Holding, UK). To examine statistically significant chromosome numbers, we have allowed ±1 deviation and 50–100 metaphase spreads were scored for each assay.

Painting probes specific for chromosome 13 (XCP13-kit, FITC; MetaSystems, GmbH) and chromosome 17 (XCP17-kit; Texas Red) (MetaSystems GmbH, Altlussheim, Germany), and multicolor probes (mFISH-24Xcyte-kit, DAPI, FITC, TexasRed, Cy3, Cy5, and DEAC; MetaSystems GmbH) were used for FISH analysis. FISH was performed according to the manufacture's protocol (MetaSystems GmbH). Briefly, both the metaphase chromosome spread and the probe were denatured with 0.07 N NaOH or 70% formamide, hybridized at 37° C for 1–4 d, and counterstained with DAPI. FISH images were captured and analyzed on the Zeiss Axio Imaging microscope (Carl Zeiss Microimaging GmbH, Jena, Germany) with Isis mBAND/mFISH imaging Software (MetaSystems GmbH).

CGH analysis. Hybridization was carried out with the BAC Array (MAC ArrayTM Karyo 4000 Component, Macrogen Co., Rockville, MD) by the Hybstation (Genomic Solutions, Ann Arbor, MI). Briefly, test DNAs, which were isolated using an isolation kit (Amersham BioSciences, Little Chalfont, UK) and Spin Column (QIAGEN Co., Tokyo, Japan), and reference DNAs (Promega Co., Madison, WI), were labeled, respectively, with Cy3 or Cy5 (BioPrimer DNA Labeling System, Invitrogen Co.), precipitated together with ethanol in the presence of Cot-1 DNA, redissolved in a hybridization mixture (50% formamide, 10% dextran sulfate, 2xSSC, 4% sodium dodecyl sulfate [SDS], pH 7), and denatured at 75° C for 10 min. After incubation at 37° C for 30 min, each mixture was applied to an array slide and incubated at 42° C for 48–72 h. After hybridization, the slides were washed in a solution of 50% formamide—2× SSC (pH 7.0) for 15 min at 50° C, in 2× SSC—0.1% SDS for 15 min at 50° C, and in a 100-mM sodium phosphate buffer containing 0.1% Nonidet P-40 (pH 8) for 15 min at room temperature, then scanned with GenePix4000A (Axon Instruments, Union City, CA). Acquired images were analyzed with MacViewer (Macrogen Instruments).

Differentiation ability. To evaluate the differentiation potential of each cell line, cells were cultured on a coverslip in each induction medium, that is, hMSC Differentiation BulletKit-Adipogenic (PT-3004, Cambrex BioScience, Inc., Walkersville, MD) for adipocyte and NPMM Bullet kit (NPMM™ BulletKit (B3209, Cambrex BioScience) for neural progenitor cells. For osteoblast, cells were treated with 0.1 μM dexamethasone (Sigma Chemical Co., St. Louis, MO), 50 μg/ml L-ascorbic acid (Sigma Chemical), and 10 mM β-glycerophosphate (Sigma Chemical) in the PLUSOID-M medium (Med-Shirotori Co.) or the POWER-EDBY10 medium (Med-Shirotori Co.) of culture medium.

After 2–4 wk, the cells were washed in phosphate-buffered saline (PBS), fixed in 4% paraformaldehyde in PBS and stained with Oil Red-O (Sigma Chemical) for detection of adipocyte, and with alkaline phosphatase staining solution containing 0.25 mg/ml naphthol AS-BI phosphate and 0.25 mg/ml Fast violet LB salt for detection of alkaline phosphatase-positive osteoblast. In immunostaining for neuron-like cells, the cells fixed with paraformaldehyde were permeabilized with methanol at −20° C for 10 min and stained with an anti-IIIβ tubulin antibody (Sigma Chemical) or anti-neurofilament antibody NF-200 (Sigma Chemical) and Texas Red-anti-mouse IgG (Southern Biotechnology Associates, Inc., Birmingham, AL) as previously described (Takeuchi et al. 1990).

Results

Changes in chromosomal number in human mesenchymal stem cell lines in prolonged culture. Immortalization of cultured cells frequently induces an abnormal chromosome number as shown in cancer cells (Duensing et al. 2000; Munger et al. 2004; Patel et al. 2004), especially at higher frequency in long-term culture. We therefore examined four cell lines, human mesenchymal stem cell (hMSC) lines immortalized with combinations of bmi-1, E6, E7, and/or hTERT genes, for chromosome instability by counting metaphase chromosomes.

All of the lines were diploid, each containing 46 up to 40 PDL including the PDL numbers of nontransfecting original MSCs (Takeda et al. 2004; Mori et al. 2005; Terai et al. 2005). For UCBTERT-21 cell, no further changes in chromosome number have been observed up to date (for PDL 133) as shown in Fig. 1*A* and *B*. In contrast, although the UBE6T-6 cell and the UE6E7T-3 cell were near diploid, both cells exhibited considerable variation in chromosome number from PDL 70 after the culture started. For example, when the assay of UE6E7T-3 cells start at PDL 62 in culture, 90% of cell population had 46 chromosomes,. but the population decreased with prolonged culturing and a population containing 44 chromosomes became dominant (43% of cell populations) at PDL 147 (Fig. 1*E*, *F*). A similar variation was also observed in UBE6T-6 cells (Fig. 1*C*, *D*).

To ascertain whether or not the changes observed were induced by transfection with HPV16E6E7, we assayed the chromosome numbers of UCB408E6E7TERT-33 cell in prolonged culture. The cell line showed similar chromosomal changes to those of the UE6E7T-3 cell, the rate of which was more rapid. At day 2 after culture by us changes became evident (PDL 68), the UCB408E6E7TERT-33 cells consisted of two distinct populations concerning chromosome number (near diploid [24%] and near tetraploid [53%]), shown in Fig. 1*G*. However, the near diploid population was unstable and decreased gradually. At PDL 81, the population became only near tetraploid, 80% of the

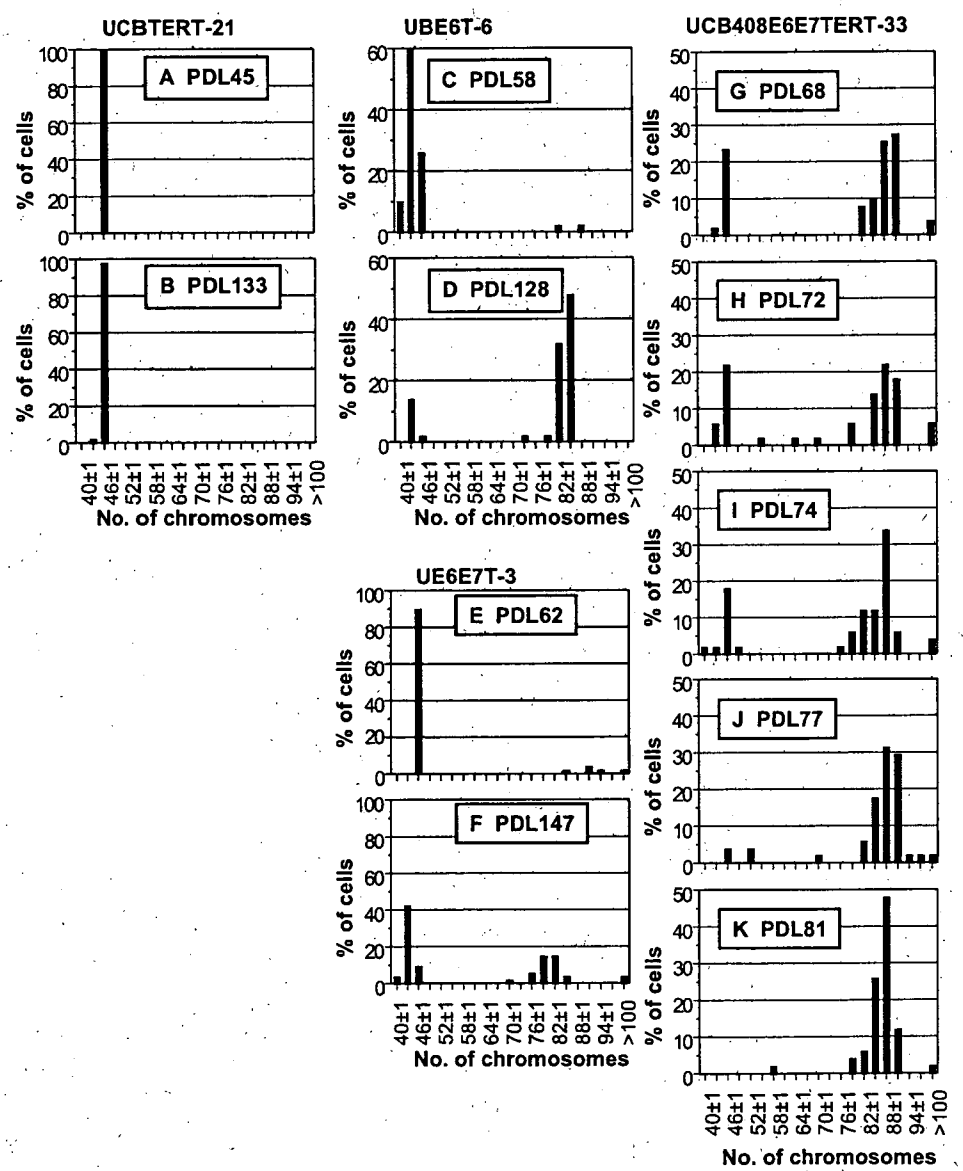

Figure 1. Changes in chromosomal numbers in prolonged cultures of four hMSC cell lines. (*A–K*) The chromosomal numbers at various culture stages were counted by DAPI staining. (*A, B*), (*C, D*), (*E, F*), and (*G–K*) represent the chromosomal numbers from UCBTERT-21, UBE6T-6, UE6E7T-3, and UCB408E6E7TERT-33, respectively. To examine statistically significant chromosomal numbers, we have allowed ±1 deviation, and 50–100 metaphase spreads were examined for each assay. *Note* the changes in chromosomal number from near 2*n* to near 4*n* in prolonged culture.

cells contain 85–92 chromosomes (Fig. 1*K*). The results indicate that UCBTERT-21 is relatively stable in chromosome number, whereas each of the oncogene-immortalized cells (UE6E7T-3, UBE6T-6, and UCB408E6E7TERT-33 cell) were unstable in chromosome numbers, which altered substantially during prolonged culture.

We next applied FISH and CGH analysis to characterize the chromosomal aberrations of the cell lines. All of the four cell lines passed for PDL 50 before examination by FISH. mFISH analysis of the UCBTERT-21 cell at PDL 52 showed normal chromosome composition (Fig. 2*A* and *B*) as observed in non-immortalized cells. The UBE6T-6 cell containing 43–45 chromosomes demonstrates losses of chromosome 13, 16, and 19 (marginal variation in chromosome 4 was observed among cells), but keeps on proliferating in chromosome number of 43–45 (Fig. 2*D*, *E*). In contrast, the UCB408E6E7TERT-33 cell showed more heterogeneity in chromosome composition with intrachromosomal and interchromosomal aberrations (data not shown). However, by mFISH analysis we were able to detect nonrandom losses of chromosome 13 in three cell lines except the UCBTERT-21 cell line. This was also confirmed by pFISH analysis using the probes specific for chromosome 13 and chromosome 17 (Fig. 2*C*, *F*). More than 97% of UCBTERT-21 cells showed two copies for chromosome 13, indicating the stability of the chromosomes in the cell line (Fig. 2*G*). The UE6E7T-3 and the UBE6T-6 cell lines with chromosome numbers of 43–45 showed only one copy of chromosome 13 in 76% of UE6E7T-3 cells and 86% of UBE6T-6 cells, respectively (Fig. 2*I*, *J*). A similar loss of chromosome 13 was also observed in 70% of UCB408E6E7TERT-33 cells, which showed three copies of chromosome 13 in near tetraploid (Fig. 2*H*). Other chromosomes, for example chromosome 17, were contained in the UCBTERT-21 and UBE6T-6 cell lines (Fig. 2*C*, *F*).

Furthermore, a significant nonrandom loss of chromosome 13 at the single cell-level observed by FISH was examined by array CGH, which samples the entire cell population. Figure 3 shows the array CGH profiles from early (*blue spots*) and late (*red spots*) stages of proliferating of each cell line. The UCBTERT-21 cell did not show any detectable differences in array CGH profiles between early and late stages (Fig. 3*A*). Although the loss of chromosome 13 had already occurred at early stages in the UBE6T-6 and the UCB408E6E7TERT-33 cell lines, in addition to the losses of chromosomes 4, 9, and 16 (Fig. 3*B*, *D*), in UE6E7T-3 the loss appeared between PDL 78 to 101 with loss of chromosome 16. The most compelling observation was that all three cell lines revealed a consistent whole loss of chromosome 13. These data are consistent with the results observed by FISH analysis. From these results, we

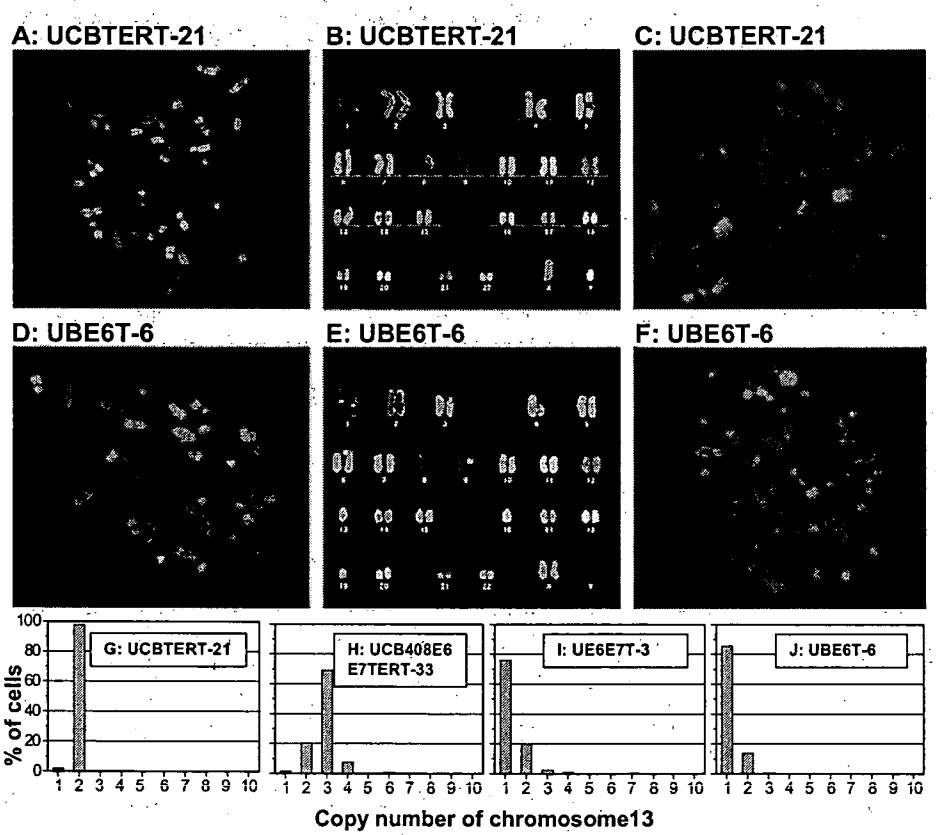

Figure 2. FISH analysis of human mesenchymal stem cell (hMSC) lines immortalized with hTERT alone, hTERT plus bm-1, HPVE6 or with hTERT plus HPVE6/E7. Multicolor FISH images of metaphase spreads (*A*, *D*), their karyotypes (*B*, *E*), and painting FISH images using DNA probes specific for chromosome 13 (*green*) and 17 (*red*) (*C*, *F*) of UCBTERT-21 (*A*, *B*, *C*) and UBE6T-6 (*D*, *E*, *F*). Quantity of chromosome 13 copy numbers in four cell lines (*G–J*). FISH signals were counted in 120~200 metaphase spreads plus interphase nuclei. UCBTERT-21 cells contained two copies of chromosome 13 and 17, and showed normal human karyotype, whereas other cells lost one copy of chromosome 13.

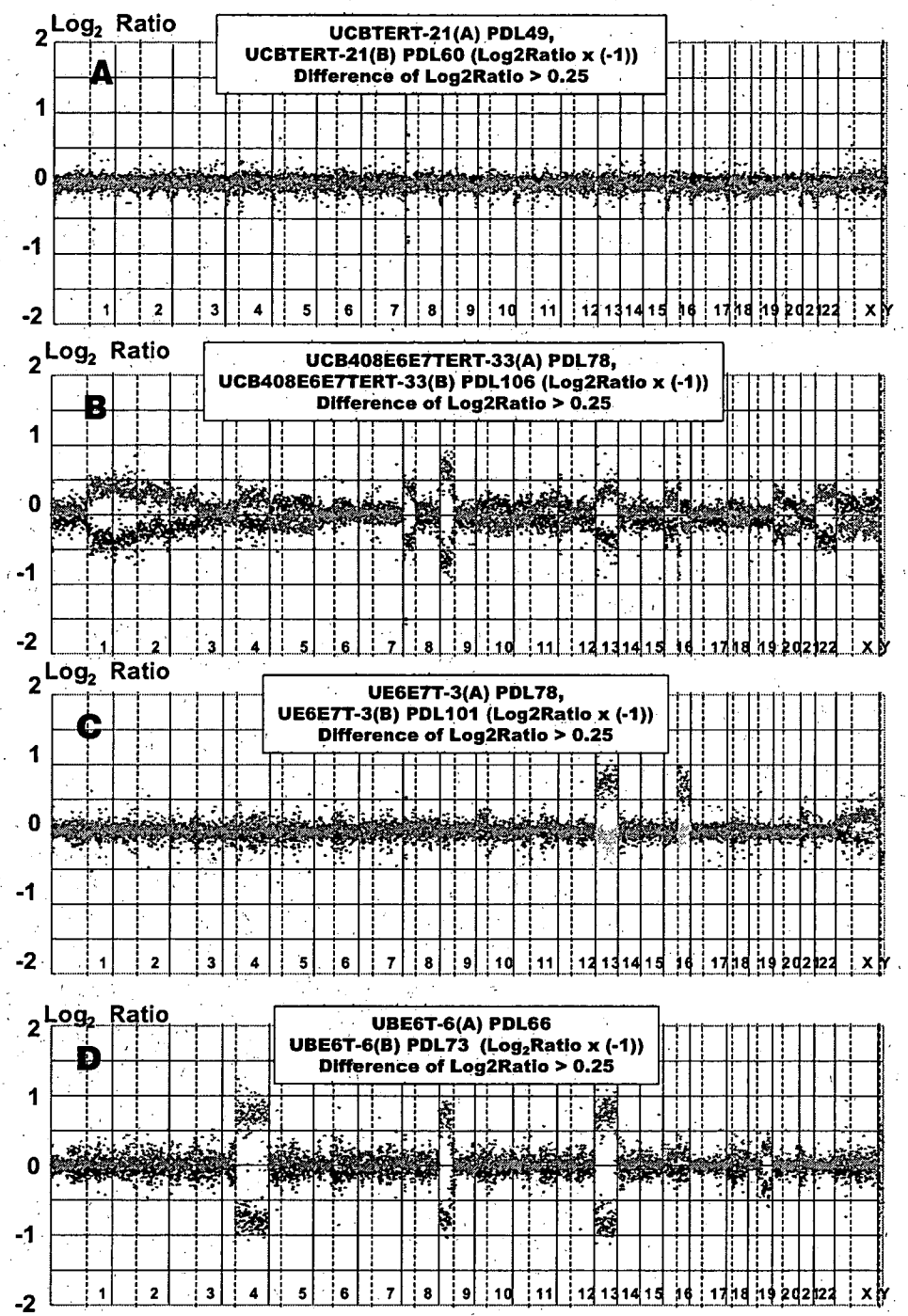

Figure 3. Array CGH profiles performed on four immortalized human mesenchymal stem cell lines at selected PDL. For each *panel*, the *X*-axis represents the 22 autosomes, the *X* and *Y* chromosomes, and the *Y*-axis shows the $\log_2$ of the fluorescence intensity ratio (cy3 [hMSCs]/cy5 [normal cell]) of all spots of the chromosome. Values above 0 (*red spots*) or values below 0 (*blue spots*) signify a loss of chromosome (chromosome regions). *Blue spots* in each *panel* indicate the $\log_2$ ratios observed at early stage in the culture of each cell line, which are overlaid with *red spots* indicated at the late stage. *Green spots* indicate the difference in value between *blue spots* and *red spot*. *Note* that in the UE6E7T-3 cell line, one copy of chromosome 13 and 16 were lost between PDL 78 and 101.

concluded that only hTERT-mediated immortalization induced little change in the chromosome numbers and chromosome structures of mesenchymal stem cells, but immortalization with Bmi-1, E6, and E7 in addition to hTERT results in chromosome instability.

Differentiation potential into lineages of immortalized mesenchymal stem cell lines. It has been reported that mesenchymal stem cells have the extensive potential to differentiate into multiple cell lineages including osteoblast, chondrocytes, adipocytes (Pittenger et al. 1999), cardiac myocytes (Makino et al. 1999), and neural cells (Pacary et al. 2006; Wislet-Gendebien et al. 2005). To evaluate whether chromosome instability of these cell lines in prolonged culture affects differentiation, cells of each cell line were stimulated in each induction medium for 2 to 4 wk. In

adipocyte-specific culture medium, all cell lines accumulated lipid-rich vacuoles in their cytoplasm within 2 wk, which were made evident by Oil Red-O staining. In particular, the UE6E7T-3 cell line showed a greater adipogenetic ability among the four cell lines (Fig. 4*Ab*). In osteoblast induction medium for 2 wk, UCB408E6E7 TERT-33 cells showed a marked increase in alkaline phosphatase expression, a marker of osteoblast, compared with those in the three other cell lines (Fig. 4*Ad*). In addition, UBE6T-6 cells in neuron induction medium reduced proliferation and displayed marked changes in morphology from being a flat-polygonal shape to taking on the characteristic neuron-like shape in which the cells develop long branching processes. Moreover, in comparing the expression patterns of characteristic neural antigens, i.e., neurofilament, III-β-tubulin, before and after induction (28 d), the pseudo-neural shaped cells showed apparent increases in immunoreactivity to both antibodies (Fig. 4*Af, Ah*),

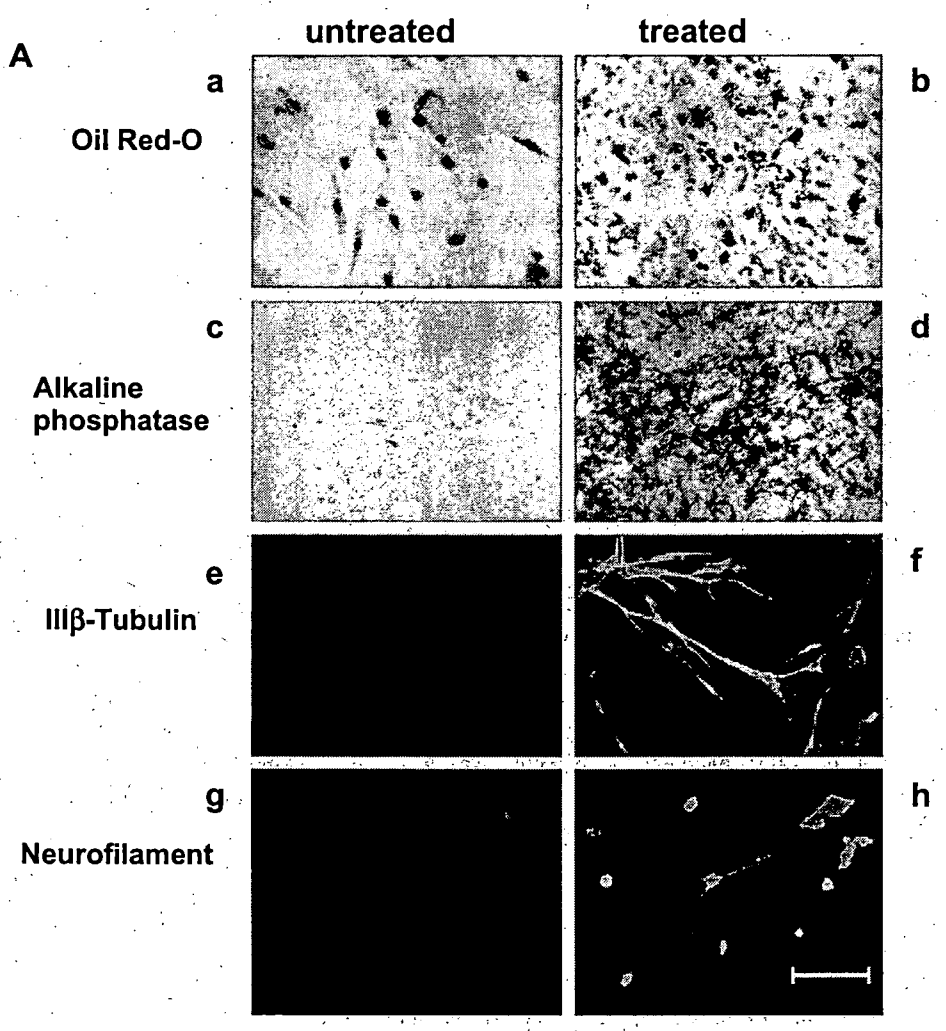

Figure 4. Differentiation potential of immortalized human mesenchymal stem cell lines into adipogenic, osteogenic, and neurogenic lineages. Adipogenesis was indicated by the accumulation of lipid stained with Oil Red-O (*Aa* and *Ab*, UE6E7T-3 cell line). Osteogenesis is indicated by the increase in alkaline phosphatase (*Ac* and *Ad*, UCB408E6E7TERT-33 cell line). Neurogenesis was shown by staining with two kinds of monoclonal antibodies to IIIβ-tubulin and neurofilament, and by shape changes of cell (*Ae–Ah*, UBE6T-6 cell line). *B*, Comparison of the differentiation potential of four cell lines whose responses to stimuli into differentiation were diverse among the cell lines. − and + indicate a response similar to an untreated cell and a weak positive response. +++ indicates a strong response shown by images of treated cells in Fig. 4*A*. (*Bar* indicates 20 μm).

B

	UCBTERT-21	UCB408E6E7TERT-33	UE6E7T-3	UBE6T-6
Oil Red-O	+	++	+++	+
Alkarine phosphatase	+	+++	+	+
IIIβ- Tubulin	-	+	+/-	+++
Neurofilament	-	++	-	++

whereas such changes were not evident with the flat-shaped cells before induction (Fig. 4*Ae*, *Ag*). Additionally, such cells did not undergo such differentiation in culture medium when cultured for as long as 30 d, although faint staining was observed. Figure 4*B* shows the overall results of differentiation potential of the four cell lines into adipogenic, osteogenic, and neurogenic lineages. These immortalized mesenchymal stem cell lines retained the ability to differentiate into three lineages, although among cell lines there are significant variations in response to lineage-specific induction.

Discussion

Attempts to clarify the mechanisms for extending the lifespan of tumor cells have been made for many years, and several genes that have effects on cellular proliferation and survival have become clear (Munger et al. 2002) in addition to the elucidation that the majority of tumor cells express telomerase (hTERT; Armanios et al. 2005). The goal of one of the series of our studies has been to establish cell lines with long lifespan and with parental properties, on the basis of genotypic and phenotypic characterizations, for application to cell-based therapy. We previously established several cell lines (Takeda et al. 2004; Mori et al. 2005; Terai et al. 2005), and the present study demonstrated that UCBTERT-21, the immortalized cell line derived from human umbilical cord blood-derived MSCs with hTERT, has a normal karyotype and has an extended lifespan by at least 133 population doublings, and has the differentiation potential into the adipocyte or osteoblast similar to parental MSCs (Terai et al. 2005), although the potential was weak but clearly positive in this study. The specific environmental cues to initiate the differentiation of hMSCs are not yet clear.

UCBTERT-21 immortalized with hTERT alone can be prolonged without inhibition of the $p16^{INK4A}$/RB pathway (Terai et al. 2005), the result of which is in agreement with reports that hTERT alone significantly extends the lifespan of human fibroblasts, epithelial, and endothelial cells (Bodnar et al. 1998; Chang et al. 2005), without the requirement for molecular alterations in p53/p21 and pRB/$p16^{INK4A}$ pathways (Milyavsky et al. 2003). However, other researchers have indicated that inactivation of the RB/p16 pathway by E7, or downregulation of p16 expression, in addition to increasing telomerase activities, is necessary for expanding the lifespan of human keratinocytes (Dickson et al. 2000; Kiyono et al. 1998). Thus, the possibility that a telomere-independent barrier may operate to prevent immortalization according to cell types has been indicated.

UCB408E6E7TERT-33, UE6E7T-3, and UBE6T-6 are hMSC-clones immortalized with HPV16E6/E7 or polycomb group oncogene Bmi-1, in combination with hTERT. Immortalization of human keratinocyte in vitro using virus-derived oncogenes such as E6 and E7 is based on initial inactivation of the p53 and/or Rb pathways, which are essential for controlling cell cycle progression in response to DNA damage or after induction tetraploidy; therefore, this gene transduction induces chromosomal abnormalities (Solinas-Toldo et al. 1997; Duensing et al. 2002; Patel et al. 2004; Schaeffer et al. 2004). The cell lines used in this study became completely immortal, yet underwent dynamic changes in their chromosome numbers in prolonged culture. Near diploid population in early passage of UCB408E6E7 TERT-33 became near-tetraploid population with prolonged culture without the appearance of intermediate populations (60–70 chromosomes/cell), and thereafter gave rise to a population having smaller numbers of chromosomes than tetraploid. Similar patterns existed, although at a slower rate, in UBE6T-6 cells and UE6E7T-3. These results suggest that HPVE6 and E7 proteins cause tetraploidy that precedes the chromosomal aberration to aneuploid in E6/E7-immotalized hMSCs, as is currently shown in several lines of evidence. For example, in vitro experiments in human cell lines (N/TERT-1 keratinocytes and HeLa cells) demonstrate that chromosome nondisjunction yields tetraploid rather than aneuploid, and that aneuploid may develop through chromosomal loss from tetraploid, although the mechanistic basis for the tetraploid formation still remains to be elucidated (Shi et al. 2005). This is also suggested from evidence that high frequency of tetraproidy is present with aneuploidy in human tumors (Olaharski et al. 2006; Sen 2000). A distinct pattern of aneuploid became apparent using dual-probe FISH and CGH analyses, in which UCB408E6E7TERT-33 cells predominantly exhibited triploid 13 and tetraploidy 17 together with other chromosomal changes as shown in Figs. 2 and 3. However, surprisingly, the loss of one copy of chromosome 13 was also seen in 70–80% of diploid UE6E7T-3 and diploid UBE6T-6 cells retaining two copies of chromosome 17. The loss occurred in PDL 50 in both UE6E7T-6 and UCB408E6E7TERT-33, and between PDL 78 and 101 in UE6E7T-3. Structural and numerical aberrations targeting chromosome 17 are often reported in tumors from various tissues (Olaharski et al. 2006), whereas the pattern that chromosome 13 is lost and chromosome 17 is stable, was common for the three cell lines in this study, indicating the possibility that the loss of chromosome 13 may play an important role in the chromosomal aberration of hMSCs to acquire growth advantages under the given culturing condition. Similar karyotypic changes were evident in cultured human embryonic stem cells, involving the gain of chromosome 17 or chromosome 12 (Carlson et al. 2000; Draper et al. 2004). It is thus conjectured that the aneuploidy developed through chromosomal loss from

diploid cells arises through different mechanisms from tetraploid intermediate.

An alternative explanation for aneuploid formation mechanism independent of tetraploid intermediate is loss of regulation in centrosome duplication, leading to abnormal centrosome amplification and multipolar spindles, resulting in aneuploidy. In addition, centrosome amplification caused by loss of p53 has been shown in cultured mouse cells (Fukasawa et al. 1996), but not in cultured human cells (Kawamura et al. 2004). However, loss of p53 and centrosome amplification has been revealed in human cancer tissue. Our preliminary examination has indicated a weak correlation between centrosome amplification and chromosome number (data not shown). Only 2.4% of UCBTERT-21 cells contained >3 centrosomes per cell, whereas 11.9% of UCB408E6E7TERT-33, 19.1% of UE6E7T-3 and 14.3% of UBE6T-6 cells contained >3 centrosomes per cell. Thus, further study is still needed to clarify the mechanism inducing chromosomal instability in immortalized hMSCs cultured over a long period.

Human mesenchymal stem cells are thought to be multipotent cells that can replicate stem cells and that can differentiate to lineages of mesenchymal tissues including bone, fat, tendon, and muscle. Our results indicated that immortalized hMSCs, except UCBTERT-21, induced changes in chromosome number over prolonged culture, but these cells have still retained the ability to both proliferate and differentiate. Immortalized UBE6T-6 cells also displayed neuron-like morphology and strong expression of the neuron-specific markers of neurofilament and III-β-tubulin. We previously demonstrated that hTERT, E7-immortalized hMSCs differentiate into neural cells in vitro on the basis of morphological changes, expression of neural markers such as nestin, neurofilament, MAP-2, Nurr1, and III-β-tubulin. Furthermore, the physiological function showed reversible calcium uptake in response to extracellular potassium concentration (Mori et al. 2005). Similar observations have been reported using rat MSCs (Wislet-Gendebien et al. 2003; Wislet-Gendebien et al. 2005; Pacary et al. 2006). In preliminary experiment of cell transplantation that 10^6 cells of UCBTERT-21 cell (PDLs 120) or UCB408E6E7TERT-33 cell (PDLs 200) were injected into nude mice subcutaneously, no tumorigenicity was observed (data not shown).

In conclusion, our study showed that the hTERT-immortalized cell line displayed normal karyotype and differentiation ability in prolonged culture. These results provide a step forward toward supplying a sufficient number of cells for new therapeutic approaches. In addition, oncogene-immortalized cell lines exhibited abnormal karyotype accompanying the preferential loss of chromosome 13 but without differential alteration during prolonged culture. Thus, the results could provide a useful model for understanding the mechanisms of the chromosomal instability and the differentiation of hMSC.

Acknowledgments This study was supported in part by a grant from the Ministry of Health, Labor and Welfare of Japan. We are grateful to Dr. T.Masui for his advice on ethics problems, and to Mr. H.Migitaka (Carl Zeiss Co., Ltd.) for his assistance with mFISH karyotype analysis. M.T. and K.T. contributed equally to this work.

References

Armanios, M.; Greider, C. W. Telomerase and cancer stem cells. Cold Spring Harbor Symp. Quant. Biol. 70:205–208; 2005.

Bodnar, A. G.; Ouellette, M.; Frolkis, M.; Holt, S. E.; Chiu, C. P.; Morin, G. B.; Harley, C. B.; Shay, J. W.; Lichtsteiner, S.; Wright, W. E. Extension of life-span by introduction of telomerase into normal human cells. Science 279:349–352; 1998.

Burns, J. S.; Abdallah, B. M.; Guldberg, P.; Rygaard, J.; Schroder, H. D.; Kassem, M. Tumorigenic heterogeneity in cancer stem cells evolved from long-term cultures of telomerase-immortalized human mesenchymal stem cells. Cancer Res. 65:3126–3135; 2005.

Carlson, J. A.; Healy, K.; Tran, T. A.; Malfetano, J.; Wilson, V. L.; Rohwedder, A.; Ross, J. S. Chromosome 17 aneusomy detected by fluorescence in situ hybridization in vulvar squamous cell carcinomas and synchronous vulvar skin. Am. J. Pathol. 157:973–983; 2000.

Chang, M. W.; Grillari, J.; Mayrhofer, C.; Fortschegger, K.; Allmaier, G.; Marzban, G.; Katinger, H.; Voglauer, R. Comparison of early passage, senescent and hTERT immortalized endothelial cells. Exp. Cell Res. 309:121–136; 2005.

Cross, S. M.; Sanchez, C. A.; Morgan, C. A.; Schimke, M. K.; Ramel, S.; Idzerda, R. L.; Raskind, W. H.; Reid, B. J. A p53-dependent mouse spindle checkpoint. Science 267:1353–1356; 1995.

Dickson, M. A.; Hahn, W. C.; Ino, Y.; Ronfard, V.; Wu, J. Y.; Weinberg, R. A.; Louis, D. N.; Li, F. P.; Rheinwald, J. G. Human keratinocytes that express hTERT and also bypass a p16(INK4a)-enforced mechanism that limits life span become immortal yet retain normal growth and differentiation characteristics. Mol. Cell Biol. 20:1436–1447; 2000.

Draper, J. S.; Smith, K.; Gokhale, P.; Moore, H. D.; Maltby, E.; Johnson, J.; Meisner, L.; Zwaka, T. P.; Thomson, J. A.; Andrews, P. W. Recurrent gain of chromosomes 17q and 12 in cultured human embryonic stem cells. Nat. Biotechnol. 22:53–54; 2004.

Duensing, S.; Lee, L. Y.; Duensing, A.; Basile, J.; Piboonniyom, S.; Gonzalez, S.; Crum, C. P.; Munger, K. The human papillomavirus type 16 E6 and E7 oncoproteins cooperate to induce mitotic defects and genomic instability by uncoupling centrosome duplication from the cell division cycle. Proc. Natl. Acad.Sci. U. S. A. 97:10002–10007; 2000.

Duensing, S.; Munger, K. The human papillomavirus type 16 E6 and E7 oncoproteins independently induce numerical and structural chromosome instability. Cancer Res. 62:7075–7082; 2002.

Fukasawa, K.; Choi, T.; Kuriyama, R.; Rulong, S.; Vande Woude, G. F. Abnormal centrosome amplification in the absence of p53. Science 271:1744–1747; 1996.

Harada, H.; Nakagawa, H.; Oyama, K.; Takaoka, M.; Andl, C. D.; Jacobmeier, B.; von, W. A.; Enders, G. H.; Opitz, O. G.; Rustgi, A. K. Telomerase induces immortalization of human esophageal keratinocytes without p16INK4a inactivation. Mol. Cancer Res. 1:729–738; 2003.

Kawamura, K.; Izumi, H.; Ma, Z.; Ikeda, R.; Moriyama, M.; Tanaka, T.; Nojima, T.; Levin, L. S.; Fujikawa-Yamamoto, K.; Suzuki, K.; Fukasawa, K. Induction of centrosome amplification and

chromosome instability in human bladder cancer cells by p53 mutation and cyclin E overexpression. Cancer Res. 64:4800–4809; 2004.

Khan, S. H.; Wahl, G. M. p53 and pRb prevent rereplication in response to microtubule inhibitors by mediating a reversible G1 arrest. Cancer Res. 58:396–401; 1998.

Kiyono, T.; Foster, S. A.; Koop, J. I.; McDougall, J. K.; Galloway, D. A.; Klingelhutz, A. J. Both Rb/p16INK4a inactivation and telomerase activity are required to immortalize human epithelial cells. Nature 396:84–88; 1998.

Makino, S.; Fukuda, K.; Miyoshi, S.; Konishi, F.; Kodama, H.; Pan, J.; Sano, M.; Takahashi, T.; Hori, S.; Abe, H.; Hata, J.; Umezawa, A.; Ogawa, S. Cardiomyocytes can be generated from marrow stromal cells in vitro. J. Clin. Invest. 103:697–705; 1999.

Milyavsky, M.; Shats, I.; Erez, N.; Tang, X.; Senderovich, S.; Meerson, A.; Tabach, Y.; Goldfinger, N.; Ginsberg, D.; Harris, C. C.; Rotter, V. Prolonged culture of telomerase-immortalized human fibroblasts leads to a premalignant phenotype. Cancer Res. 63:7147–7157; 2003.

Mori, T.; Kiyono, T.; Imabayashi, H.; Takeda, Y.; Tsuchiya, K.; Miyoshi, S.; Makino, H.; Matsumoto, K.; Saito, H.; Ogawa, S.; Sakamoto, M.; Hata, J.; Umezawa, A. Combination of hTERT and bmi-1, E6, or E7 induces prolongation of the life span of bone marrow stromal cells from an elderly donor without affecting their neurogenic potential. Mol. Cell Biol. 25:5183–5195; 2005.

Munger, K.; Baldwin, A.; Edwards, K. M.; Hayakawa, H.; Nguyen, C. L.; Owens, M.; Grace, M.; Huh, K. Mechanisms of human papillomavirus-induced oncogenesis. J. Virol. 78:11451–11460; 2004.

Munger, K.; Howley, P. M. Human papillomavirus immortalization and transformation functions. Virus Res. 89:213–228; 2002.

Okamoto, T.; Aoyama, T.; Nakayama, T.; Nakamata, T.; Hosaka, T.; Nishijo, K.; Nakamura, T.; Kiyono, T.; Toguchida, J. Clonal heterogeneity in differentiation potential of immortalized human mesenchymal stem cells3. Biochem. Biophys. Res. Commun. 295:354–361; 2002.

Olaharski, A. J.; Sotelo, R.; Solorza-Luna, G.; Gonsebatt, M. E.; Guzman, P.; Mohar, A.; Eastmond, D. A. Tetraploidy and chromosomal instability are early events during cervical carcinogenesis. Carcinogenesis 27:337–343; 2006.

Pacary, E.; Legros, H.; Valable, S.; Duchatelle, P.; Lecocq, M.; Petit, E.; Nicole, O.; Bernaudin, M. Synergistic effects of CoCl(2) and ROCK inhibition on mesenchymal stem cell differentiation into neuron-like cells. J. Cell Sci. 119:2667–2678; 2006.

Patel, D.; Incassati, A.; Wang, N.; McCance, D. J. Human papillomavirus type 16 E6 and E7 cause polyploidy in human keratinocytes and up-regulation of G2-M-phase proteins. Cancer Res. 64:1299–1306; 2004.

Pittenger, M. F.; Mackay, A. M.; Beck, S. C.; Jaiswal, R. K.; Douglas, R.; Mosca, J. D.; Moorman, M. A.; Simonetti, D. W.; Craig, S.; Marshak, D. R. Multilineage potential of adult human mesenchymal stem cells. Science 284:143–147; 1999.

Saito, M.; Handa, K.; Kiyono, T.; Hattori, S.; Yokoi, T.; Tsubakimoto, T.; Harada, H.; Noguchi, T.; Toyoda, M.; Sato, S.; Teranaka, T. Immortalization of cementoblast progenitor cells with Bmi-1 and TERT. J. Bone Miner. Res. 20:50–57; 2005.

Schaeffer, A. J.; Nguyen, M.; Liem, A.; Lee, D.; Montagna, C.; Lambert, P. F.; Ried, T.; Difilippantonio, M. J. E6 and E7 oncoproteins induce distinct patterns of chromosomal aneuploidy in skin tumors from transgenic mice. Cancer Res. 64:538–546; 2004.

Sen, S. Aneuploidy and cancer. Curr. Opin. Oncol. 12:82–88; 2000.

Shi, Q.; King, R. W. Chromosome nondisjunction yields tetraploid rather than aneuploid cells in human cell lines. Nature 437:1038–1042; 2005.

Solinas-Toldo, S.; Durst, M.; Lichter, P. Specific chromosomal imbalances in human papillomavirus-transfected cells during progression toward immortality. Proc. Natl. Acad. Sci. U. S. A 94:3854–3859; 1997.

Takeda, Y.; Mori, T.; Imabayashi, H.; Kiyono, T.; Gojo, S.; Miyoshi, S.; Hida, N.; Ita, M.; Segawa, K.; Ogawa, S.; Sakamoto, M.; Nakamura, S.; Umezawa, A. Can the life span of human marrow stromal cells be prolonged by bmi-1, E6, E7, and/or telomerase without affecting cardiomyogenic differentiation? J. Gene Med. 6:833–845; 2004.

Takeuchi, K.; Kuroda, K.; Ishigami, M.; Nakamura, T. Actin cytoskeleton of resting bovine platelets. Exp. Cell Res. 186:374–380; 1990.

Terai, M.; Uyama, T.; Sugiki, T.; Li, X. K.; Umezawa, A.; Kiyono, T. Immortalization of human fetal cells: the life span of umbilical cord blood-derived cells can be prolonged without manipulating p16INK4a/RB braking pathway. Mol. Biol. Cell 16:1491–1499; 2005.

Wislet-Gendebien, S.; Hans, G.; Leprince, P.; Rigo, J. M.; Moonen, G.; Rogister, B. Plasticity of cultured mesenchymal stem cells: switch from nestin-positive to excitable neuron-like phenotype. Stem Cells 23:392–402; 2005.

Wislet-Gendebien, S.; Leprince, P.; Moonen, G.; Rogister, B. Regulation of neural markers nestin and GFAP expression by cultivated bone marrow stromal cells. J. Cell Sci. 116:3295–3302; 2003.

Zheng, L.; Lee, W. H. The retinoblastoma gene: a prototypic and multifunctional tumor suppressor. Exp. Cell Res. 264:2–18; 2001.

Am J Physiol Gastrointest Liver Physiol 293: G1089–G1098, 2007.
First published September 20, 2007; doi:10.1152/ajpgi.00187.2007.

A role of Wnt/β-catenin signals in hepatic fate specification of human umbilical cord blood-derived mesenchymal stem cells

Yoko Yoshida,[1] Takashi Shimomura,[1] Tomohiko Sakabe,[1] Kyoko Ishii,[1] Kazue Gonda,[1] Saori Matsuoka,[1] Yumi Watanabe,[1] Kazuko Takubo,[2] Hiroyuki Tsuchiya,[1] Yoshiko Hoshikawa,[1] Akihiro Kurimasa,[1] Ichiro Hisatome,[3] Taro Uyama,[4] Masanori Terai,[4] Akihiro Umezawa,[4] and Goshi Shiota[1]

[1]*Division of Molecular and Genetic Medicine, Department of Genetic Medicine and Regenerative Therapeutics, Graduate School of Medicine, Tottori University;* [2]*Division of Oral and Maxillofacial Biopathological Surgery, Department of Medicine of Sensory and Motor Organs, Faculty of Medicine, Tottori University;* [3]*Division of Regenerative Medicine, Department of Genetic Medicine and Regenerative Therapeutics, Graduate School of Medicine, Tottori University; and* [4]*Department of Reproductive Biology and Pathology, National Research Institute for Child Health and Development, Tokyo, Japan*

Submitted 30 April 2007; accepted in final form 7 September 2007

Yoshida Y, Shimomura T, Sakabe T, Ishii K, Gonda K, Matsuoka S, Watanabe Y, Takubo K, Tsuchiya H, Hoshikawa Y, Kurimasa A, Hisatome I, Uyama T, Terai M, Umezawa A, Shiota G. A role of Wnt/β-catenin signals in hepatic fate specification of human umbilical cord blood-derived mesenchymal stem cells. *Am J Physiol Gastrointest Liver Physiol* 293: G1089–G1098, 2007. First published September 20, 2007; doi:10.1152/ajpgi.00187.2007.—Human umbilical cord blood-derived mesenchymal stem cells (UCBMSCs) are expected to be an excellent source of cells for transplantation. In addition, the stem cell plasticity of human UCBMSCs, which can transdifferentiate into hepatocytes, has been reported. However, the mechanisms involved remain to be clarified. To identify the genes and/or signals that are important in specifying the hepatic fate of human UCBMSCs, we analyzed gene expression profiles during the hepatic differentiation of UCBMSCs with human telomerase reverse transcriptase, UCBMSCs immortalized by infection with a retrovirus carrying telomerase reverse transcriptase, but whose differentiation potential remains unchanged. Efficient differentiation was induced by 5-azacytidine (5-aza)/hepatocyte growth factor (HGF)/oncostatin M (OSM)/fibroblast growth factor 2 (FGF2) treatment in terms of function as well as protein expression: 2.5-fold increase in albumin, 4-fold increase in CCAAT enhancer-binding protein α, 1.5-fold increase in cytochrome p450 1A1/2, and 8-fold increase in periodic acid-Schiff staining. Consequently, we found that the expression of Wnt/β-catenin-related genes downregulated, and the translocation of β-catenin was observed along the cell membrane and in the cytoplasm, although some β-catenin was still in the nucleus. Downregulation of Wnt/β-catenin signals in the cells by Fz8-small interference RNA treatment, which was analyzed with a Tcf4 promoter-luciferase assay, resulted in similar hepatic differentiation to that observed with 5-azacytidine/HGF/OSM/FGF2. In addition, the subcellular distribution of β-catenin was similar to that of cells treated with 5-azacytidine/HGF/OSM/FGF2. In conclusion, the suppression of Wnt/β-catenin signaling induced the hepatic differentiation of UCBMSCs, suggesting that Wnt/β-catenin signals play an important role in the hepatic fate specification of human UCBMSCs.

mesenchymal stem cell; Wnt/β-catenin signaling pathway; hepatic differentiation

HUMAN UMBILICAL CORD BLOOD (UCB) has been reported to contain stem/progenitor cells at concentrations greater than or equal to those in bone marrow and adult peripheral blood (28, 30). In addition, the use of UCB entails few ethical problems, and even now most UCB is regarded as medical waste in delivery rooms. Although bone marrow is an important source of stem cells, its use has several disadvantages: aspirating bone marrow from patients is an invasive procedure, and the capacity of stem cells to differentiate decreases with the donor's age (7). UCB-cell transplantation for various blood diseases has recently been successful, with a lower incidence of graft-vs.-host disease than that seen in many conventional treatments (18). Thus UCB is considered useful for therapeutic applications.

It has long been thought that the differentiation potential of adult stem cells is limited to their germ layer of origin, but recent studies have demonstrated that adult stem cells are more plastic than once believed (1, 20–22, 47). Mesenchymal stem cells (MSCs) can differentiate into several lineages including osteoblasts, chondrocytes, and adipocytes. Recently, in vivo transplantation studies showed that MSCs can differentiate into endodermal cell types as well as most mesodermal and neuroectodermal types (15). Human MSCs from bone marrow and UCB-derived MSCs (UCBMSCs) can differentiate into hepatocytes in vitro (41, 24, 25). UCBMSC may become an important alternative source of cells for transplantation; however, the hepatic differentiation of MSCs is not efficient enough for clinical use. Therefore, the molecular mechanism of hepatic differentiation should be clarified. Newly established UCBMSCs with human telomerase reverse transcriptase (UCBTERT) proliferated for >120 population doublings, and the characteristics of the cells including differentiation potential remained unchanged (46). Therefore, UCBTERT cells provide a powerful model for the application of stem cell-based therapies.

Adult stem cells, under certain microenvironmental conditions, give rise to cell types besides the cell type of origin, indicating that they can switch cell fate, a feature termed "stem cell plasticity" (23). An alternative mechanism to induce cell plasticity could be the cell fusion of a bone marrow-derived cell with a nonhematopoietic cell (19). Although use of the Cre/loxP system revealed that some hepatocytes from bone marrow-derived cells are really produced by cell fusion in vivo (2), in vitro hepatic differentiation of MSCs demonstrated that

Address for reprint requests and other correspondence: G. Shiota, Division of Molecular and Genetic Medicine, Dept. of Genetic Medicine and Regenerative Therapeutics, Graduate School of Medicine, Tottori Univ., Yonago 683-8504, Japan (e-mail: gshiota@grape.med.tottori-u.ac.jp).

The costs of publication of this article were defrayed in part by the payment of page charges. The article must therefore be hereby marked "*advertisement*" in accordance with 18 U.S.C. Section 1734 solely to indicate this fact.

stem cell plasticity really exists (24, 25). In addition, we previously reported that the hepatic differentiation of UCB cells as well as cell fusion occurred simultaneously in vivo (45). Since cells generated from cell fusions may be more likely to undergo transformation, hepatocytes differentiated from UCB cells in vitro, which do not mediate cell fusion, are a reliable cell source for regenerative medicine. We therefore attempted to identify the genes and/or signals that regulate the hepatic differentiation of human UCBMSCs.

MATERIALS AND METHODS

Materials. Fibroblast growth factor 2 (FGF2), hepatocyte growth factor (HGF), and oncostatin M (OSM) were purchased from PeproTech EC (London, UK). Recombinant Wnt-3A was obtained from R&D Systems. Mesenchymal stem cell growth medium (MSCGM, PT-3001) and SYTOX green nucleic acid stain were purchased from Cambrex Bio Science. 5-Azacytidine (5-aza) was obtained from Nacalai Tesque (Kyoto, Japan). Anti-human serum albumin antibody (A 6684), anti-C/EBPα antibody (sc-61), and anti-CYP1A1/1A2 (AB1255), and Cy3-conjugated secondary antibody (AP132C) were purchased from Sigma Aldrich (St. Louis, MO), Santa Cruz Biotechnology (Santa Cruz, CA), and Chemicon International, respectively.

Culture of UCBTERT-21 cells. Human UCBMSCs, the life span of which was prolonged by infection with a retrovirus encoding human telomerase reverse transcriptase (hTERT), designated UCBTERT-21 cells (46), were used. All cultures were maintained at 37°C in a humidified atmosphere containing 95% air and 5% CO_2. To induce the hepatic differentiation of UCBTERT-21 cells in vitro, we added several cytokines to the culture media. UCBTERT-21 cells were plated into six-well plates at 2×10^4 cells/well and cultured overnight to allow cell attachment. To induce hepatic differentiation, UCBTERT-21 cells were cultured in MSCGM containing 1 μM 5-aza for 24 h and then cultured in MSCGM containing 10% FBS, 10 ng/ml FGF2, 20 ng/ml HGF, and 20 ng/ml OSM for 3 wk with special reference to Refs. 25, 29, and 41. The medium was changed weekly (Fig. 1). Hepatic differentiation was assessed by reverse transcription-polymerase chain reaction (RT-PCR), immunostaining, periodic acid-Schiff (PAS) staining, and urea assay.

RNA extraction and RT-PCR analysis. Total RNA was extracted from UCBTERT-21 cells by using a Total RNA Isolation kit (Promega, Madison, WI). cDNA samples were synthesized from 1 μg of total RNA by using a Super Script II first-strand synthesis system (Invitrogen, Carlsbad, CA) with a-oligo(dT)-adaptor primer according to the manufacturer's instructions. The cDNA preparation template was used for subsequent PCR amplification by using *Taq* DNA polymerase. The primers for albumin, CCAAT/enhancer-binding protein α (C/EBPα), CCAAT/enhancer-binding protein β (C/EBPβ), cytochrome p4501A1 (CYP1A1), cytochrome p4501A2 (CYP1A2), phosphoenolpyruvate carboxykinase (PEPCK), and GAPDH were as follows: albumin forward primer, 5′-TTGGAAAAATCCCACTGCAT-3′; albumin reverse primer, 5′-CTCCAAGCTGCTCAAAAAGC-3′; C/EBPα forward primer, 5′-CACGAAGCACGATCAGTCCAT-3′; C/EBPα reverse primer, 5′-CGCACATTCACATTGCACAAG-3′; C/EBPβ forward primer, 5′-GCCAAGAAGACCGTGGACA-3′; C/EBPβ reverse primer, 5′-GCCAAGAAGACCGTGGACA-3′; CYP1A1 forward primer, 5′-ACCATGACCAGAAGCTATGGGT-3′; CYP1A1 reverse primer, 5′-TTAACACCTTGTCGATAGCACCA-3′; CYP1A2 forward primer, 5′-ACCATGACCCAGAGCTGTGG-3′; CYP1A2 reverse primer, 5′-TCACTCAAGGGCTTGTTAAT-3′ PEPCK forward primer, 5′-CAGGCAGCTGAAGAAGTATGA-3′, PEPCK reverse primer, 5′-AACCGTCTTGCTTTCGATCCT-3′, GAPDH forward primer, 5′-GTCTTCTCCACCATGGAGAAGGCT-3′; GAPDH reverse primer, 5′-CATGCCAGTGAGCTTCCCGTTCA-3′. Albumin was amplified at 95°C for 2 min, with denaturing at 95°C for 30 s, annealing at 58°C for 30 s, and extension at 72°C for 30 s for 35 cycles. GAPDH was amplified at 95°C for 2 min, with denaturing at 95°C 30 s, annealing at 60°C for 30 s, and extension at 72°C for 30 s for 30 cycles. The PCR products were analyzed by electrophoresis with a 2% agarose gel and stained with ethidium bromide. The intensity of the UV-light illuminated bands was measured by ImageJ (http://rsb.info.nih.gov/ij/) and was expressed after being normalized to GAPDH. Control RNA from normal adult liver was obtained when a patient with colon cancer metastasis underwent partial hepatectomy under informed consent.

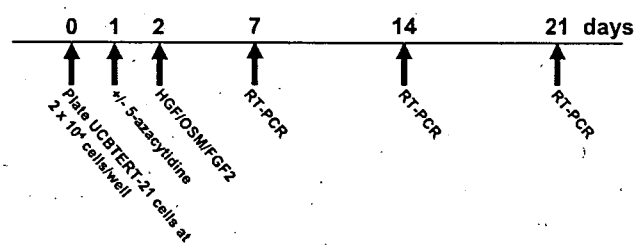

Fig. 1. Induction of hepatic differentiation of umbilical cord blood-derived mesenchymal stem cells with human telomerase reverse transcriptase (UCBTERT-21) cells. Experimental protocol. UCBTERT-21 cells were transferred into 6-well plates at 2×10^4 cells/well. The cells were cultured in mesenchymal stem cell growth medium (MSCGM) with or without 1 μM 5-azacytidine (5-aza) or not for 24 h and then cultured in MSCGM containing 20 ng/ml hepatocyte growth factor (HGF), 20 ng/ml oncostatin M (OSM), and/or 10 ng/ml fibroblast growth factor 2 (FGF2) for 3 wk. The culture medium was exchanged weekly. Total RNA was extracted from the UCBTERT-21 cells for RT-PCR.

Real-time quantitative PCR analysis. The cDNA template was amplified by use of a LightCycler (Roche). β-Actin was employed as an internal reference gene to normalize cDNA input. The mRNA expression levels of β-catenin, PP2A, and frizzled 8 (Fz8) were defined as the ratio of the value of each gene product to that of the β-actin product. The primers were as follows: albumin forward primer, 5′- TGTTGCATGAGAAAACGCCA-3′; albumin reverse primer, 5′- GTCGCCTGTTCACCAAGGAT-3′; Fz8 forward primer, 5′-TCTGGTGGGTGATCTTGTCG-3′; Fz8 reverse primer, 5′-AGCACCGCGATGGACTTGAC-3′; β-actin forward primer, 5′-CACTCTTCCAGCCTTCCTTCC-3′; β-actin reverse primer, 5′-CGTACAGGTCTTTGCGGATGTC-3′. The real-time PCR assays were performed with SYBR green (Roche) according to the manufacturer's instructions.

PAS staining for glycogen. Cells were fixed with PBS containing 4% formaldehyde for 20 min, permeabilized with PBS containing 0.1% Triton X-100 for 10 min, and incubated in the presence or absence of 1 mg/ml diastase for 1 h at 37°C. Samples were then oxidized in 1% periodic acid for 5 min, treated with Schiff's reagent for 15 min, rinsed three times in a sodium sulfite solution (0.5% sodium sulfite, 0.05 N HCl), and rinsed another three times in H_2O. Sections were assessed under a light microscope.

Urea assay. UCBTERT-21 cells at 1×10^5 cells/well were cultured, and the cell density was adjusted weekly. After 3 wk, 3×10^4 cells were incubated with 5 mM ammonium chloride, and the amount of urea secreted into the medium was measured every 24 h for up to 96 h. Urea concentrations were determined with a QuantiChrom urea assay kit (BioAssay Systems) according to the manufacturer's instructions.

Immunocytochemistry. Cultures were collected by enzymatic methods and were plated onto coverslips. The coverslips were fixed in PBS containing 4% formaldehyde for 20 min and permeabilized with PBS containing 0.2% Triton X-100 for 10 min. Samples were blocked with goat serum for 20 min and then incubated with anti-human serum albumin, anti-human C/EBPα, anti-CYP1A1/1A2, or anti-β-catenin antibodies, followed by Vectastain ABC Systems (Vector Laboratories, Burlingame, CA) or Cy3-conjugated secondary antibody. Hematoxylin or SYTOX green was utilized for nuclear counterstaining. The

coverslips were mounted with Gel/Mount, and the sections were assessed under a light microscope or fluorescence microscope.

DNA microarrays. RNA was extracted from UCBTERT-21 cells treated with or without 5-aza/HGF/OSM/FGF2 on *day 7* by use of an RNeasy mini kit (Qiagen), followed by digestion with RNase-free DNase (Qiagen). DNA microarray analysis was performed using AceGene human oligo chip 30k 1 chip version (Hitachi Software Engineering, Yokohama, Japan), which contains the oligonucleotide probe sets for 30,000 human genes. The intensity of fluorescence of each probe was measured with a Fuji FLA-8000 scanner (FujiPhoto Film, Tokyo, Japan) and quantified using Array Gauge software (FujiPhoto Film). The expression of each gene was compared between UCBTERT-21 cells treated with and without 5-aza/HGF/OSM/FGF2.

Transfection of siRNA. The Fz8 small interference RNA (siRNA; Fzd8-siRNA, cat. SI02646413) and nonsilencing siRNA control (negative control siRNA, cat. 1022563) were purchased from Qiagen. UCBTERT-21 cells were transfected with siRNA in multiwell plates by using RNAiFect transfection reagent (Qiagen). A mixture of 1 μg siRNA, 100 μl Buffer EC-R, and 6 μl RNAiFect transfection reagent was incubated for 15 min at room temperature. One hundred microliters of the mixture and 300 μl of medium containing 10% FBS were incubated with the cells for 6 h. The effect of mRNA silencing was confirmed by real-time quantitative PCR analysis.

Gene reporter assay. The plasmid Tcf4-CMVpro-Luc contains three copies of the optimal Tcf motif CCTTTGATC upstream of the CMV promoter that drives the expression of luciferase (Fig. 4*B*) (38). The CMV promoter sequence was inserted into pGL3-Basic vector (Promega). The plasmid pRL-TK (Promega) was used as an internal control. Transient transfection was performed using RNAiFect transfection reagent. As a positive control, 100 ng/ml of Wnt-3a was added 24 h after transfection. At 48 h after transfection, the cell lysates were used for gene reporter assays with the Dual-Luciferase reporter assay system (Promega).

RESULTS

Optimal conditions for hepatic differentiation. UCBTERT-21 cells are suitable for this study because they proliferate clonally and expand for a prolonged number of passages, and, importantly, introduction of the hTERT gene did not change the characteristics of the cells (46). UCBTERT-21 cells were expanded in six-well plates at 2.0×10^4 cells/well. The cells were cultured first with or without 5-aza for 24 h and then with a combination of HGF, OSM, and FGF2 for 3 wk (Fig. 1). Albumin mRNA expression was evaluated by RT-PCR with seven combinations of these agents: 5-aza/HGF/OSM/FGF2, 5-aza/HGF/OSM, 5-aza/HGF, 5-aza, HGF/OSM/FGF2, HGF/OSM, and HGF compared with 10% FBS. On *day 0*, UCBTERT-21 cells expressed little albumin mRNA, and MSCGH scarcely expressed albumin mRNA without 5-aza or cytokines. The combination of 5-aza/HGF/OSM/FGF2 for 3 wk was more effective than the other seven combinations (data not shown).

To more precisely examine albumin mRNA expression, real-time PCR was performed using RNA obtained under optimal conditions and from the controls (Fig. 2*A*). The expression level of albumin mRNA after treatment with 5-aza/HGF/OSM/FGF2 was almost eightfold higher than that in MSCGM containing 10% FBS. We investigated whether UCBTERT-21 cells subjected to theses conditions expressed hepatocyte-specific proteins by immunocytochemistry. The expression of albumin was upregulated in the cells treated with 5-aza/HGF/OSM/FGF2, especially in the cells that proliferated at high density (Fig. 2*B*, *a* and *e*). Staining of C/EBPα was also increased, and the nuclei of treated cells were stained strongly (Fig. 2*B*, *b* and *f*). CYP1A1/2 staining was weak in untreated cells, but it was more intense in treated cells (Fig. 2*B*, *c* and *g*). The cells positive for CYP1A/2 were larger than those negative for CYP1A/2. The presence of stored glycogen, as determined by PAS staining, was observed in treated cells (Fig. 2*B*, *d* and *h*). Untreated cells did not show the ability to synthesize glycogen. When pretreated with diastase to digest glycogen, treated cells stained negative for glycogen (data not shown).

The level of cells positive for hepatic marker proteins and PAS staining in UCBTERT-21 cells treated with 5-aza/HGF/OSM/FGF2 significantly increased, compared with the control: a 2.5-fold increase in albumin, 4-fold increase in C/EBPα, 1.5-fold increase in CYP1A1/1A2, and 8-fold increase in PAS staining were induced by this treatment ($P < 0.01$, $P < 0.01$, $P < 0.05$, and $P < 0.01$, respectively, Fig. 2*C*).

Secretion of urea by the cells was measured every 24 h after the addition of 5 mM ammonium chloride. Urea in the medium became detectable at 24 h in both treated and untreated cells and increased thereafter, tending to be higher in the treated cells at 48 and 72 h. At 96 h, the production of urea was significantly greater in the treated cells compared with the control ($P < 0.05$, Fig. 2*D*).

The expression levels of albumin, C/EBPα, c/EBPβ, CYP1A1, Cyp1A2, and PEPCK were examined by RT-PCR (Fig. 2*E*). The expression levels of albumin, C/EBPα, C/EBPβ, CYP1A1, CYP1A2, and PEPCK were strongly induced in UCBTERT cells treated with 5-aza/HGF/OSM/FGF2. However, the expression levels of albumin, C/EBPα, C/EBPβ, CYP1A1, CYP1A2, and PEPCK in adult normal liver cells were 1.7-fold, 2.0-fold, 1.1-fold, 0.7-fold, and 3.5-fold greater than that of the treatment with 5-aza/HGF/OSM/FGF2. These findings suggest that UCBTERT cells treated with 5-aza/HGF/OSM/FGF2 were still immature compared with adult mature hepatocytes.

Genes that are associated with hepatic differentiation of human MSCs. We investigated the genes whose expression changed during the treatment with 5-aza/HGF/OSM/FGF2. Total RNA extracted from cells, that were treated with 5-aza/HGF/OSM/FGF2 or control medium for one wk, was examined by microarray analysis. We found that the expression levels of many Wnt signal-related molecules were downregulated in the treated cells, compared with the untreated cells (Table 1). The expression level of CTNNB1 (β-catenin) and many of the Fz family genes was decreased, including the expression level of Fz8. On the other hand, the expression level of CTNNBIP1 (ICAT), which inhibits Wnt signaling (44), increased by 2.4-fold. The expression of PPP2CA (protein phosphatase 2 catalytic subunit), which has a positive role in Wnt signal transduction (36), decreased. Conversely, the expression level of PPP2R1B (protein phosphatase regulatory subunit), which inhibits Wnt signaling (27), increased. Real-time RT-PCR analysis showed that β-catenin, PPA2CA, and Fz8 were downregulated in their expression (Fig. 3*A*); treatment with 5-aza/HGF/OSM/FGF2 reduced the expression of β-catenin, PPA2CA, and Fz8 to 82, 78, and 25%, respectively, of the control. Fz8 maintained its expression at ~20–40% of the control level during the course of hepatic differentiation of UCBMSC (Fig. 3*B*).

Subcellular distribution of β-catenin during hepatic localization. We investigated the subcellular localization of β-catenin in UCBTERT-21 cells by immunocytochemistry. β-Cate-

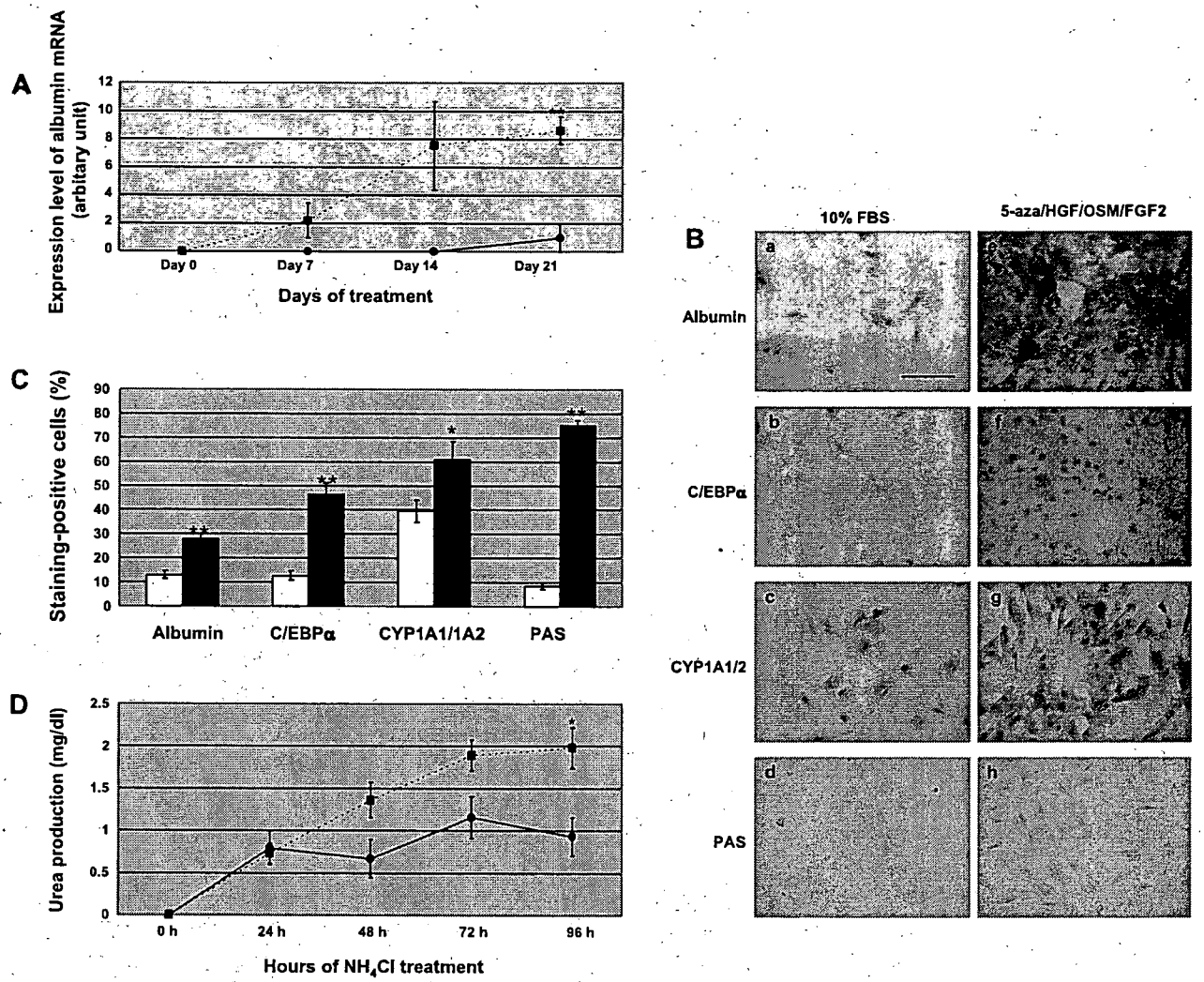

Fig. 2. Hepatic differentiation of UCBTERT-21 cells. *A*: expression of the albumin gene evaluated by quantitative real-time RT-PCR. The level of albumin gene expression is shown as a ratio of that in the control on *day 21*. ●, 10% FBS (control); ■, 10% FBS with 5-aza/HGF/OSM/FGF2. Data are expressed as means ± SE of 3 experiments. $^{**}P < 0.01$ compared with the control. *B*: induction of hepatic specific genes in UCBTERT-21 cells on *day 21* was analyzed by cytochemistry. *a–d*, 10% FBS; *e–h*, 10% FBS with 5-aza/HGF/OSM/FGF2. Cells were immunostained with anti-albumin (*a, e*), anti-CCAAT enhancer-binding protein α (C/EBPα) (*b, f*), and anti-cytochrome p450 1A1/2 (CYP1A1/1A2) (*c, g*) antibodies. Glycogen stored in the cells was stained by periodic acid-Schiff (PAS) stain (*d, h*). Scale bar, 100 μm. *C*: efficiency of hepatic differentiation of UCBTERT-21 cells on *day 21*. Open bars, 10% FBS (control); solid bars, 10% FBS with 5-aza/HGF/OSM/FGF2. Data are expressed as means ± SE of 6 experiments. $^{**}P < 0.01$, $^{*}P < 0.05$, compared with control. *D*: urea production in the culture medium of differentiated UCBTERT-21 cells. ●, 10% FBS (control); ■, 10% FBS with 5-aza/HGF/OSM/FGF2. Data are expressed as means ± SE of 6 experiments. $^{*}P < 0.05$, compared with control. *Fig. 2 (Continues).*

nin has dual roles, as an adhesion molecule at the plasma membrane and as a key intermediate in the canonical Wnt signaling pathway. On activation of the Wnt cascade, β-catenin in the cytosolic soluble pool becomes stabilized and then translocates into the nucleus where it coactivates transcription factors of the TCF/LEF family (4). On *day 7* after the start of treatment, β-catenin was mostly located in the nuclei of the cells (Fig. 3*C*). On *day 14* and *day 21*, β-catenin was also observed along the cell membrane and in the cytoplasm, but some was still in the nucleus (Fig. 3*C*). The translocation of β-catenin was observed during hepatic cell differentiation (5, 31). Thus the changes in β-catenin localization may be important during hepatic differentiation of progenitor cells.

Knockdown of the genes of MSC leading to hepatic differentiation. Since the expression levels of β-catenin, PP2CA, and Fz8 were downregulated during the course of hepatic differentiation of UCBTERT-21 cells, the suppressive effect of Fz8, which is essential for Wnt/β-catenin signaling (4), on hepatic differentiation was examined by using RNA interference. First, we confirmed that the expression level of Fz8 mRNA in Fz8-siRNA-transfected cells was decreased to 60% of that at 0 h at 48 h after transfection (Fig. 4*A*). To investigate the effect of Fz8 knockdown on β-catenin/TCF4 transcriptional activity, we performed a luciferase reporter assay with pTcf4-CMVpro-Luc, using pRL-TK as an internal control (Fig. 4*B*). Treatment with Wnt-3a enhanced luciferase activity,